Stem Cell Reports
Article

ISSCR

OPEN ACCESS

Improved hematopoietic stem cell transplantation upon inhibition of natural killer cell-derived interferon-gamma

Lorena Lobo de Figueiredo-Pontes,[1,13] Miroslava K. Adamcova,[2,3,13] Srdjan Grusanovic,[2,3,4] Maria Kuzmina,[2,4] Izabela Aparecida Lopes,[1] Amanda Fernandes de Oliveira Costa,[1] Hong Zhang,[5] Hynek Strnad,[6] Sanghoon Lee,[7] Alena Moudra,[8] Anna T. Jonasova,[8] Michal Zidka,[9,10] Robert S. Welner,[5,11] Daniel G. Tenen,[5,12,14,*] and Meritxell Alberich-Jorda[2,3,14,*]

[1]Hematology Division, Department of Medical Images, Hematology, and Clinical Oncology, Ribeirão Preto Medical School, University of São Paulo, Ribeirão Preto, SP 14048-900, Brazil

[2]Department of Hemato-oncology, Institute of Molecular Genetics of the Czech Academy of Sciences, Prague 142 00, Czech Republic

[3]Childhood Leukaemia Investigation Prague, Department of Pediatric Haematology and Oncology, 2nd Faculty of Medicine, Charles University in Prague, University Hospital Motol, Prague 150 06, Czech Republic

[4]Faculty of Science, Charles University, Prague 128 00, Czech Republic

[5]Harvard Stem Cell Institute, Harvard Medical School, Boston, MA 02115, USA

[6]Department of Genomics and Bioinformatics, Institute of Molecular Genetics of the Czech Academy of Sciences, Prague 142 00, Czech Republic

[7]Department of Systems Biology, The University of Texas MD Anderson Cancer Center, Houston, TX 77030, USA

[8]1st Department of Medicine - Department of Haematology, First Faculty of Medicine, Charles University in Prague and General University Hospital, Prague 120 00, Czech Republic

[9]Orthopaedic Department CLPA-Mediterra, Prague 190 00, Czech Republic

[10]3rd Medical Faculty, Charles University, Prague 100 00, Czech Republic

[11]Department of Medicine, Division Hematology/Oncology, University of Alabama at Birmingham, Birmingham, AL 35294, USA

[12]Cancer Science Institute, National University of Singapore, Singapore 117599, Singapore

[13]These authors contributed equally

[14]Co-senior author

*Correspondence: daniel.tenen@nus.edu.sg (D.G.T.), alberich@img.cas.cz (M.A.-J.)

https://doi.org/10.1016/j.stemcr.2021.06.008

SUMMARY

Hematopoietic stem cell transplantation (HSCT) is a frequent therapeutic approach to restore hematopoiesis in patients with hematologic diseases. Patients receive a hematopoietic stem cell (HSC)-enriched donor cell infusion also containing immune cells, which may have a beneficial effect by eliminating residual neoplastic cells. However, the effect that donor innate immune cells may have on the donor HSCs has not been deeply explored. Here, we evaluate the influence of donor natural killer (NK) cells on HSC fate, concluded that NK cells negatively affect HSC frequency and function, and identified interferon-gamma (IFNγ) as a potential mediator. Interestingly, improved HSC fitness was achieved by NK cell depletion from murine and human donor infusions or by blocking IFNγ activity. Thus, our data suggest that suppression of inflammatory signals generated by donor innate immune cells can enhance engraftment and hematopoietic reconstitution during HSCT, which is particularly critical when limited HSC numbers are available and the risk of engraftment failure is high.

INTRODUCTION

Hematopoietic stem cell transplantation (HSCT) is the only curative therapy for many hematologic diseases where hematopoiesis needs to be replaced by healthy hematopoietic cells. The success of HSCT mostly depends on the speed and quality of the hematopoietic recovery in the early post-transplantation phase. Although the main goal of the procedure is to inject hematopoietic stem cells (HSCs) with high self-renewal potential to fully reestablish hematopoiesis, blood- or bone marrow-derived donor stem cell sources also contain committed progenitors and immune cells. Presence of immune cells in the donor sample has been associated with prevention of infections (Chen et al., 2006; Storek et al., 1997; Tomblyn et al., 2010) and graft-versus-tumor effects (Venstrom et al., 2010; Wagner et al., 2005). However, besides these well-known effects, it may be hypothesized that immune cells from the graft can also affect donor HSC properties and modify engraftment.

Recent evidence has elucidated that hematopoietic cells, particularly T lymphocytes, known for their ability to trigger inflammatory responses, may directly or indirectly affect the function of hematopoietic stem and progenitor cells (Geerman and Nolte, 2017). Hirata and colleagues showed that bone marrow (BM) cluster of differentiation (CD) 4 memory T cells and memory regulatory T cells (Tregs) coordinate each other to generate extracellular adenosine via CD39 and CD73, maintaining HSC quiescence (Hirata et al., 2018). Similarly, memory CD8$^+$ T cells support the maintenance of HSCs in the BM (Geerman et al., 2018). Nevertheless, in a transplantation setting using a xenotransplant model, it was demonstrated that donor-derived activated memory T cells present in unfractionated umbilical cord blood (UCB) were associated with reduced HSC engraftment in comparison with CD34$^+$

fractionated UCB. This effect was attributed to tumor necrosis factor alpha (TNFα) cytokine produced by these memory T cells and was reverted by TNFα receptor inhibition (Wang et al., 2017). On the contrary, several studies showed that, when HSCs are limiting, memory CD8$^+$ T cells have a beneficial effect on HSPC engraftment, both in allogeneic and autologous transplantation (Russell et al., 2015; Touzot et al., 2015; Triplett et al., 2015). Altogether, these observations highlight the relevance of the immune cells present in the graft, and question their presence as an advantage or disadvantage in a transplantation setting.

Natural killer (NK) cells are lineage-specific lymphocytes with effector functions of cytotoxicity and cytokine production. NK cell activity depends on a dynamic balance between the expression of activating receptors (which recognize stress-induced ligands on infected or tumor cells), inhibitory receptors (which predominantly bind major histocompatibility complex [MHC] class I molecules), and cytokine receptors (Kim et al., 2005; Vivier et al., 2008). Upon stimulation, NK cells are also able to produce cytokines such as interleukin (IL)-1, IL-3, IL-4, IL-5, IL-6, granulocyte colony-stimulating factor (G-CSF), granulocyte-macrophage colony-stimulating factor (GM-CSF), macrophage colony-stimulating factor (M-CSF), TNFα, and IFNγ, which can potentially influence the properties of self-renewal, apoptosis, mobilization, and differentiation of HSCs and determine different outcomes to hematopoiesis (Baldridge et al., 2010; Buza-Vidas et al., 2006; Schuettpelz and Link, 2013; Zhang and Lodish, 2008). However, besides its cytotoxic effects mediated by HLA missense recognition signals in HSCT, a potential role in the regulation of HSC functions in transplantation has not been explored.

In the transplant setting, the immune content of the graft may be activated or modified by the pre-transplant conditioning regimen based on chemotherapy and/or radiotherapy (Joncker et al., 2010; Mehta et al., 2015). Both T and NK cells can recognize and kill residual tumor cells, but while the activation of T cells by the recipient's antigen-presenting cells often causes graft-versus-host disease (GvHD), a potentially lethal complication of the procedure, NK cells are capable of eliminating tumor cells without being involved in GvHD (Raziuddin et al., 2002; Ruggeri et al., 2002). Thus, differently from T cells, NK cells have been traditionally recognized as transplant helpers. However, the effects of donor NK cells based on their secretory potential on HSC function during transplantation so far remain unknown.

In the present study, we showed that NK cells impair HSC function in culture and *in vivo*. Our results demonstrated that NK cells from the graft negatively influence HSC engraftment and hematopoietic recovery upon BM transplantation. By using CCAAT-enhancer-binding protein gamma (*Cebpg*) conditional knockout (KO) mice, we revealed that the effect is mediated by the production of cytokines such as IFNγ. Importantly, addition of IFNγ-blocking antibodies to HSC-NK co-cultures prevented the NK detrimental effect on HSC, and administration of IFNγ-blocking antibodies during the early phase post transplant enhanced human HSC engraftment and hematopoietic reconstitution. Altogether, our study demonstrates that donor NK cells present in the graft can negatively affect the early post-transplantation phase, and that modulating inflammatory signals such as IFNγ can contribute to improved engraftment during HSCT.

RESULTS

NK cells reduce HSC maintenance and function in culture

To investigate potential HSC alterations when exposed to NK cells, we developed a co-culture system of sorted murine HSCs and NK cells (Figure 1A). HSCs were defined by cell surface markers as lineage negative (Lin$^-$), Sca-1$^+$, c-kit$^+$, CD48$^-$, CD150$^+$, and NK cells as Lin$^-$, CD3$^-$, and NK1.1$^+$. Co-cultures were established on an OP9 stromal cell layer with appropriate HSC culture conditions in the presence of the NK cell activating cytokine IL-2 (Figure 1A). Using fluorescence-activated cell sorting (FACS) analysis, we observed a reduction of phenotypically defined HSCs after 4 days of culture when NK cells were present. This reduction was dependent on the NK/HSC ratio, and was more profound as the number of NK cells in culture increased (Figures 1B and S1). Next, we performed colony culture assays to assess whether the presence of NK cells would compromise HSC function *in vitro* (Figure 1C). Colony-forming units were enumerated at day 10 of culture, and we observed a significant reduction in the presence of NK cells. Similar to our previous result, the number of colonies was reduced in a dose-dependent manner according to the increasing number of NK cells (Figure 1D). Altogether, these experiments suggest that NK cells can negatively influence HSC frequency and function in culture.

NK cells affect murine HSC repopulation capacity *in vivo*

Next, we investigated whether NK cells alter HSC properties *in vivo*. Sorted CD45.1/2 HSCs were cultured alone or co-cultured with CD45.2 NK cells (ratio of 1 × 10^5 NK cells to 1,500 HSCs) overnight, and injected into lethally irradiated CD45.2 mice (Figure 2A). Importantly, we enumerated HSCs post overnight culture and prior to transplantation, and observed a reduced number of remaining viable HSCs in cell suspensions containing NK cells compared

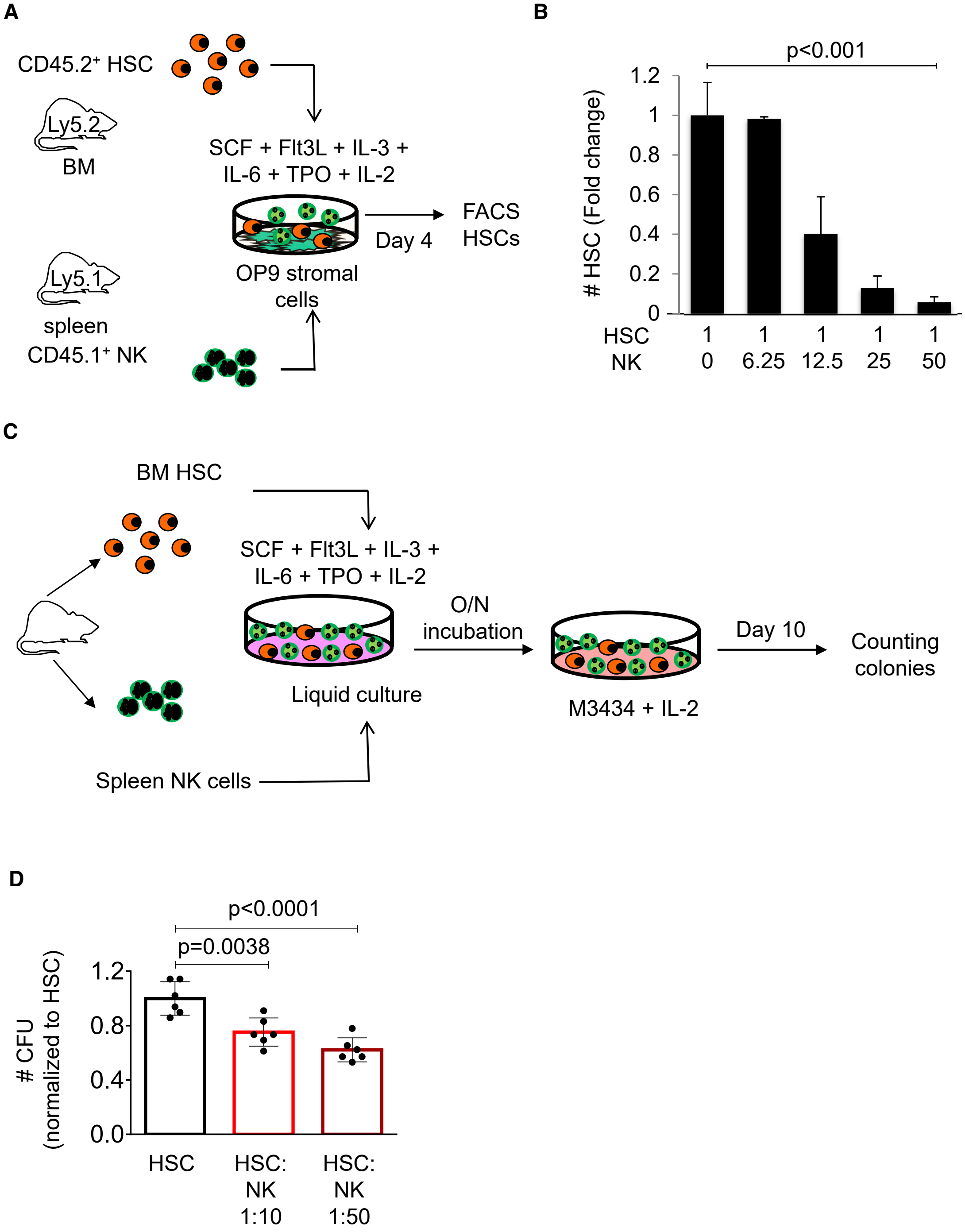

Figure 1. NK cells reduce HSC maintenance and function in culture

(A) Graphical representation of the experimental design. Co-cultures were established in stem cell medium containing stem cell factor (SCF), Flt3-ligand, IL-3, IL-6, thrombopoietin (TPO), and IL-2 over an OP9 stromal cell layer using sorted BM CD45.2$^+$ HSCs (lin$^-$ c-Kit$^+$ Sca-1$^-$ CD48$^-$ CD150$^+$) and SP CD45.1$^+$ NK cells (Ter119$^-$ CD19$^-$ CD4$^-$ CD8$^-$ CD3$^-$ NK1.1$^+$). Days of culture are indicated. HSCs were enumerated by FACS analysis.

(B) Quantification of HSCs recovered from 4-day cultures by FACS analysis. Y axis indicates the absolute number of HSCs. X axis indicates presence (+) or absence (−) of NK cells in culture (ratios are indicated). Values and error bars indicate medians ±SEM. n = 3 biological samples in each condition. Jonckheere-Terpstra trend test was used to assess statistical significance (p value is indicated).

(legend continued on next page)

with suspensions without NK cells (Figure 2B). Nine weeks after transplantation, peripheral blood analysis demonstrated a reduction of CD45.1/2 cells when HSCs were exposed to NK cells prior to transplantation (Figure 2C). However, NK-exposed HSCs showed no skewing to myeloid, B, or T cell differentiation (Figures 2D and S2A). Next, we assessed the long-term effects of exposing HSCs to NK cells overnight, and observed a significantly reduced percentage of CD45.1/2 cells in blood, BM, and spleen (SP) of recipient mice 16 weeks after transplantation (Figure 2E). Importantly, homing assays demonstrated that addition of NK cells to the donor cell preparations did not alter HSC homing (Figure S2B). Together, these results demonstrated that NK cells negatively affect the numbers of functional HSCs, and, therefore, reduce their hematopoietic reconstitution ability compared with non-exposed HSCs.

NK cells present in murine BM grafts compromise stem cell function

Since our previous results demonstrated that co-culturing NK cells and HSCs lead to HSC impaired repopulation capacity, we hypothesized that NK cells and HSC co-habitation in the BM donor samples could cause intrinsic changes to HSC function. To test this hypothesis, we first assessed whether removal of NK cells from total BM would improve short-term reconstitution. Whole BM from CD45.1 mice was submitted to immunomagnetic NK1.1 (NK cells) or immunoglobulin (Ig) G (control) depletion and injected into lethally irradiated CD45.2 mice (Figure 3A). NK cell depletion was verified by flow cytometry analysis prior to transplantation (Figure S3A). Donor chimerism after 8 weeks of transplant showed that NK cell depletion from the BM improved the short-term engraftment ability of HSC (Figure 3B). Next, we performed limiting dilution transplantation assays following the same NK cell depletion strategy (Figure 3A), and assessed whether the long-term HSC properties would be also affected by NK cells. Limiting dilution transplantation assays allowed us to measure the frequency of repopulating units, which reflects the number of functional HSCs. Positive engraftment was defined as >0.3% and at least two-lineage reconstitution. We observed a 5-fold increased number of functional HSCs when NK cells were removed prior to transplantation ($p < 0.000804$) (Figure 3C). Further, NK cell depletion from the BM graft did not affect the differentiation pattern of lymphoid or myeloid lineages (Figures 3D and S3B). Altogether, our results demonstrated that NK cell removal from donor BM in murine transplantation assays improves the short-term as well as long-term transplantation outcome without altering the lineage hematopoietic recovery.

NK cells negatively affect human CD34$^+$ cells *in vitro* and *in vivo*

Next, we assessed whether the effects that NK cells have on murine HSCs would translate to human primary samples. Human HSCs were isolated from BM (CD34$^+$), co-cultured overnight in the presence of human IL-2, with or without human NK cells (CD19$^-$ CD8$^-$ CD4$^-$ CD3$^-$ CD56$^+$), and placed in semi-solid media supplemented with human IL-2 (same strategy as in Figure 1C). The number of colonies was enumerated at day 10 of culture, in which we observed colony-forming unit (CFU) reduction in the presence of NK cells, suggesting that NK cells can harm human HSCs' ability to form colonies (Figure 4A). Since NK cell depletion during murine BM transplantation assays improved hematopoietic engraftment and reconstitution, we next performed experiments to determine how depletion of NK cells from human grafts could affect HSCT. NK cell-depleted (CD56) or non-depleted (IgG) human BM samples were transplanted into sublethally irradiated immunodeficient NOD.Cg-*Prkdc*^{scid}*Il2rg*^{tm1Wjl}/SzJ (NSG) mice at different doses (Figure 4B). CD3 antibodies were included in the depletion cocktail to remove human T cells from the graft, to prevent GvHD. The efficiency of immunomagnetic depletion of NK cells was demonstrated by flow cytometry analysis prior to BM transplantation (Figure S4). The engraftment and contribution of human BM cells to the hematopoietic system of recipient mice was determined by the percentage of human CD45$^+$ cells in blood, BM, and SP 14 weeks after transplantation. We observed that ablation of NK cells from human BM grafts had a positive effect in the transplants, leading to better reconstitution and engraftment of human cells in recipient mice (Figure 4C). These positive effects after NK cell removal were visible in different cell doses and in two independent experiments using different healthy BM grafts; however, no statistical significance was reached and we could only observe a tendency in our human transplantation assays. Altogether, *in vitro* and *in vivo* experiments suggest that NK cells can impair HSC function, which can be restored by NK cell depletion.

Cebpg KO NK cells exhibit milder effects than wild-type NK cells on HSC function

Next, since the transcription factor C/EBPγ was related to NK cell function and *Cebpg*-deficient NK cells were severely

(C) Experimental design of *in vitro* colony culture assays.

(D) Quantification of colonies at day 10 of culture. Y axis indicates the number of CFU relative to the HSC counts. X axis indicates cells present in the semi-solid cultures. Two different HSC/NK cell ratios were used as indicated. Data indicate mean ± SD of three independent biological triplicates. Each dot represents one culture well. Two-tailed Student's t test was used to assess statistical significance (p values are indicated).

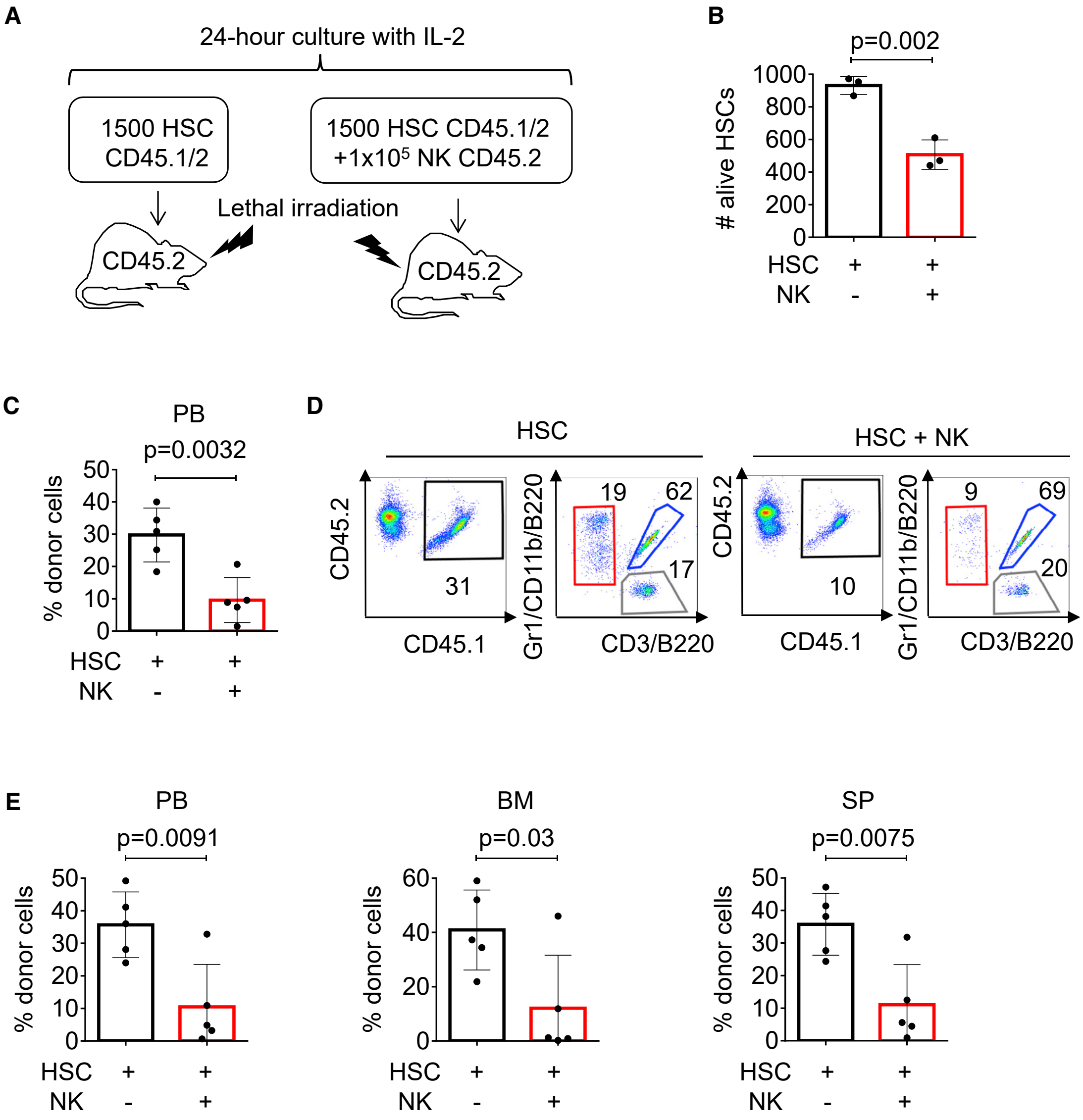

Figure 2. NK cell exposure compromises HSC engraftment *in vivo*

(A) Experimental strategy for NK and HSCT assays. HSCs from C57BL/6 CD45.1/2 mice were purified by sorting, cultured in the presence or absence of NK cells (Ter119$^-$ CD19$^-$ CD4$^-$ CD8$^-$ CD3$^-$ NK1.1$^+$) obtained from C57BL/6 CD45.2 mice, and injected into lethally irradiated CD45.2 recipient animals in a ratio of 10^5 NK cells to 10^3 HSCs per mouse.

(B) Number of HSCs assessed by FACS. Y axis indicates number of alive Hoechst 33,258$^-$ HSCs after overnight incubation. X axis indicates culture conditions.

(C) Flow cytometry analysis of recipient mice peripheral blood 9 weeks after transplantation. Y axis indicates the percentage of donor-derived CD45.1/2$^+$ cells. X axis indicates different culture conditions.

(D) Representative flow cytometry plots of recipient mice peripheral blood 9 weeks after transplantation. Plots show CD45.1 versus CD45.2 expression in HSC and HSC + NK transplanted mice. Black box indicates the percentage of CD45.1/2$^+$ donor-derived cells and the gate used to analyze tri-lineage contribution: red box indicates the percentage of myeloid cells (Gr1/CD11b$^+$), blue box the percentage of B cells (B220$^+$), and gray box the percentage of T cells (CD3$^+$). See also Figure S2.

(E) FACS analysis of peripheral blood (PB), BM, and SP isolated from recipient mice 16 weeks after transplantation. Y axes indicate the percentage of donor CD45.1/2$^+$ cells and X axes indicate distinct culturing conditions. Five animals were included in each group. All data represent mean ± SD from one representative experiment out of three. Two-tailed Student's t test was used to assess statistical significance (p values are indicated).

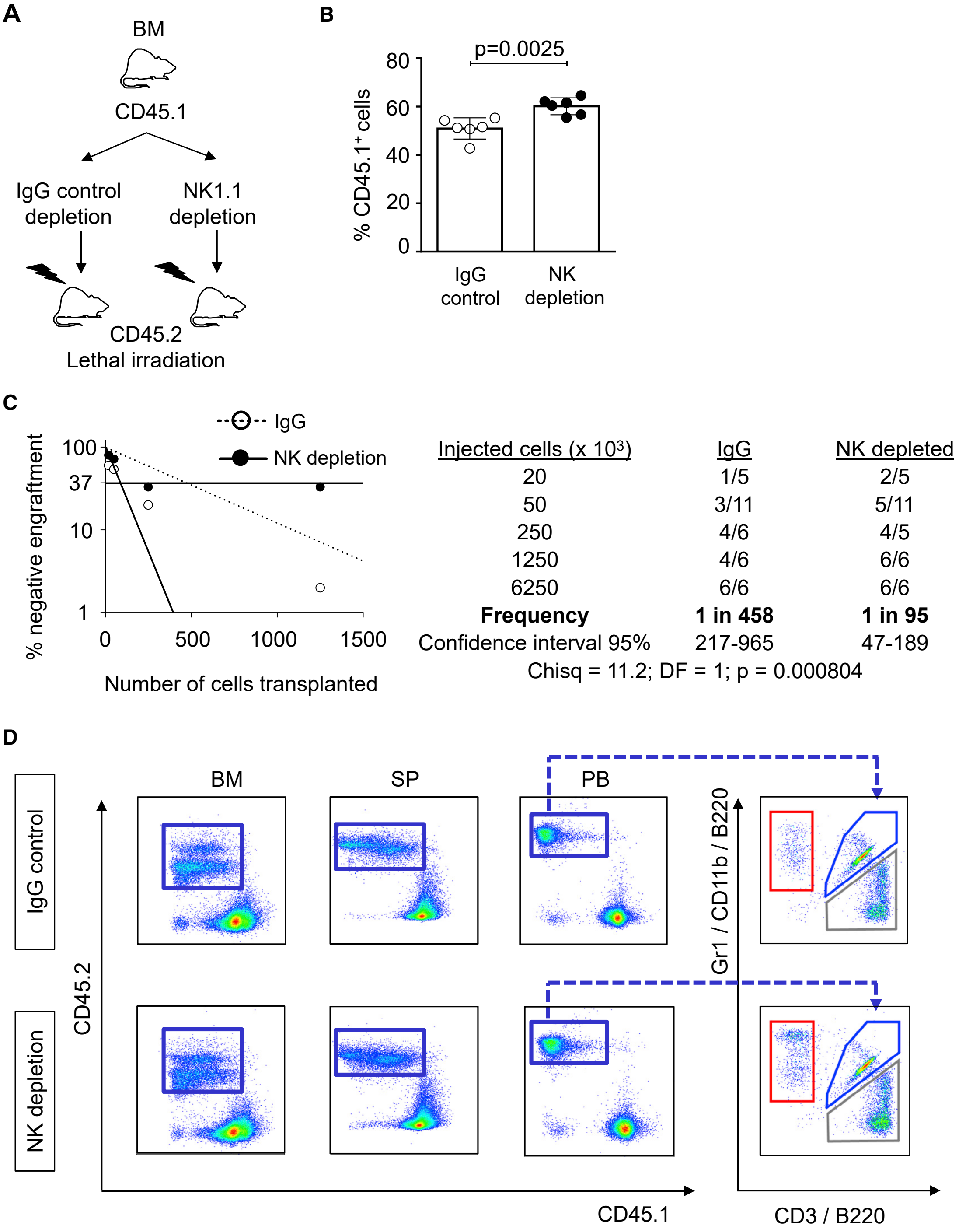

Injected cells (x 10^3)	IgG	NK depleted
20	1/5	2/5
50	3/11	5/11
250	4/6	4/5
1250	4/6	6/6
6250	6/6	6/6
Frequency	**1 in 458**	**1 in 95**
Confidence interval 95%	217-965	47-189

Chisq = 11.2; DF = 1; p = 0.000804

Figure 3. NK cell depletion from murine BM improves stem cell function

(A) Overview of the experimental strategy for the BM transplantation assay after NK cell depletion (NK1.1) or irrelevant IgG depletion (control). Upon depletion, cells were injected into lethally irradiated CD45.2 animals.

(B) FACS analysis of peripheral blood of recipient mice. Y axis indicates the percentage of donor CD45.1$^+$ cells 9 weeks after transplantation. X axis indicates IgG control or NK cell depletion. In each group 6.25 × 10^6 cells were transplanted into recipient mice. Six animals were included in each group. All data represent mean ± SD from one representative experiment out of two. Two-tailed Student's t test was used to assess statistical significance (p value is indicated). See also Figure S3.

(legend continued on next page)

impaired in their cytotoxicity against target cells (Kaisho et al., 1999), we investigated the effect of *Cebpg*-deficient NK cells on HSC function. First, we analyzed *Cebpg* expression in distinct hematopoietic populations, and observed that *Cebpg* mRNA expression is higher in the lymphoid than myeloid lineage and BM HSPCs (Figure 5A). The highest *Cebpg* mRNA expression was detected in NK cells. Next, we took advantage of a *Cebpg* conditional KO mouse model generated in our laboratory (Kardosova et al., 2018). *Cebpg* conditional KO mice were crossed to Vav-iCre transgenic mice in order to induce *Cebpg* excision in the hematopoietic compartment. We generated *Cebpg*$^{\text{flox/flox}}$ Vav-iCre^{-} (wild-type [WT]) and *Cebpg*$^{\text{flox/flox}}$ Vav-iCre^{+} (*Cebpg* KO) mice. Absence of *Cebpg* was confirmed by mRNA quantification in BM and SP (Figure 5B). Frequency of *Cebpg* KO NK cells was not altered, and expression of NK cell-activating receptors was similar in KO and WT mice (Figures S5A and S5B). However, purified *Cebpg* KO NK cells stimulated with IL-2 had lower cytotoxicity against murine YAC-1 lymphoma cells (Figure S5C), indicating that *Cebpg*-deficient NK cells exhibit reduced functionality. Next, we assessed whether *Cebpg* KO NK cells would be able to affect HSC colony-forming abilities. Interestingly, we observed that the deleterious effect of NK cells was abolished when *Cebpg* was absent in NK cells, demonstrating that nonfunctional NK cells do not harm HSCs *in vitro* (Figure 5C). Further, we investigated whether *Cebpg* KO NK cells would impair HSC function *in vivo*. Using similar HSC and NK cell co-culture conditions as previously described in Figure 2A, HSCs were isolated from WT CD45.1/2 mice and NK cells were isolated from either WT or *Cebpg* KO mice (CD45.2), co-cultured overnight, and were injected into lethally irradiated CD45.2 recipients. Prior to transplantation, we enumerated HSCs in the co-cultures and observed that *Cebpg* KO NK cells do not have the ability to reduce the number of viable HSCs, in contrast to WT NK cells (Figure S5D). Flow cytometric analysis of recipient mice showed that the effect of *Cebpg*-deficient NK cells was much milder than the effect of WT NK cells (Figure 5D). This partial rescue was present 9 and 16 weeks after transplantation, and the contribution to myeloid, B cells, and T cells was similar in all three groups (Figure S5D). Together, our *in vitro* and *in vivo* experiments demonstrated that *Cebpg* KO mice produce normal numbers of NK cells, which are functionally impaired, and do have milder effects than WT NK cells during HSCT.

The regulatory effects of NK cells on stem cells are cytokine mediated

Since *Cebpg*-deficient NK cells were not able to affect the hematopoietic reconstitution of recipient mice, we investigated potential mediators of HSC regulation by NK cells by comparing the gene expression profile of WT and *Cebpg* KO NK cells. NK cells were sorted from WT and *Cebpg* KO mice, cultured overnight with IL-2 or vehicle control, and gene expression profiling was performed (E-MTAB-5604). Using the LIMMA package to assess differential gene expression, we identified 1,074 genes deregulated in WT versus *Cebpg* KO NK cells ($p < 0.05$), and 1,316 genes deregulated in IL-2-treated WT versus IL-2-treated *Cebpg* KO NK cells ($p < 0.05$). Using prediction analysis of microarrays, we identified and selected 84 probe sets, corresponding to 75 genes, significantly up- or downregulated in WT and *Cebpg* KO NK cells in the presence or absence of IL-2 (Table S1). Figure 6A shows a heatmap and hierarchical clustering according to expression of the 84 probe sets. These results identified an NK signature characterized by a set of genes targeted upon NK activation. Pathway analysis of differentially expressed mRNA demonstrated cell pathways associated to deregulated genes in WT versus *Cebpg* KO NK cells (Table S2). Since we observed more pronounced effects on HSC function when NK cells were exposed to IL-2, we further performed pathway analysis in IL-2 treated samples. Our results demonstrated that the IFNγ signaling pathway was the top pathway among deregulated genes, suggesting that it might contribute to NK cell effects on HSC (Table 1). To gain further insights into the mechanisms mediating the NK cell effects, we analyzed differentially expressed genes between WT and *Cebpg*-deficient NK cells treated with IL-2. Figure 6B shows a heatmap and hierarchical clustering according to expression of 29 genes present in the NK signature. Within the

---

(C) Panels indicate results from limiting dilution competitive repopulation unit assays. (Left) Logarithmic plot showing the percentage of negative recipients transplanted with different cell doses of murine BM depleted with NK1.1 Ab (black dots) or control IgG Ab (white dots). Only recipients at 16 weeks with engraftment of CD45.1 cells $\geq 0.1\%$ and contribution to all lineages (T cells, B cells, and granulocytes) higher than 1% were considered responders. (Right) Table showing the number of responders and the total number of recipients transplanted per cell dose. Frequencies of HSCs (1:95 in NK1.1-depleted BM transplants versus 1:458 in IgG-depleted control, p = 0.000804) were calculated according to Poisson statistics using ELDA software based on data from two independent experiments (Chisq, chi-square test).

(D) Representative flow cytometry dot plots showing the percentages of CD45.1^{+} donor cells (blue boxes, Y axes) and CD45.2^{+} host cells (X axes). Plots show BM, SP, and PB of mice injected with IgG-depleted control (upper panels) and NK-depleted (lower panels) BM cells 16 weeks after transplant. The panels on the right refer to gated CD45.1^{+} PB and indicate T (gray box), B (blue box), and myeloid (red box) cells, as determined by the use of antibodies against CD3, B220, and Gr1/CD11b, respectively.

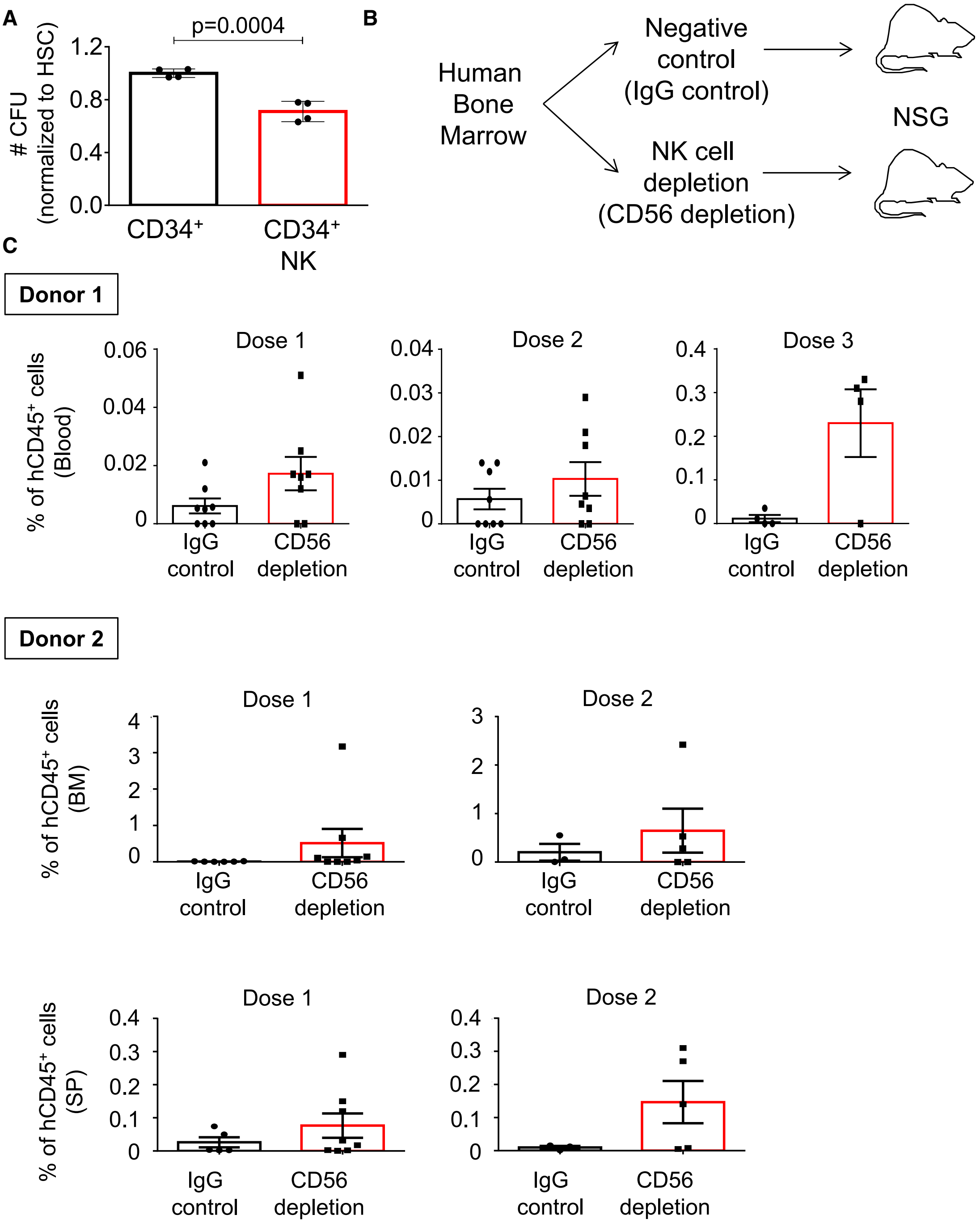

Figure 4. Engraftment of human BM stem cells is optimized by NK cell removal

(A) Human CFU assays of CD34$^+$ cells with or without NK cells (ratio 1:10), after overnight culture in the presence of human IL-2. Y axis indicates the mean CFU number ±SD from two distinct human BM samples relative to CD34$^+$ cells cultured alone. X axis indicates the distinct culture conditions. Each black dot indicates values for one culture well. Two-tailed Student's t test was used to assess statistical significance (p value is indicated).

(B) Illustration of the experimental strategy. Human BM samples depleted with antibodies against CD3 and IgG (negative control) or against CD3 and CD56 (NK cell depletion) were transplanted into sublethally irradiated NOD.Cg-*Prkdc*^{scid}*Il2rg*^{tm1Wjl}/SzJ (NSG) mice at different doses.

(legend continued on next page)

upregulated genes in the *Cebpg* KO NK cells, we identified lactotransferrin (*Ltf*), lysozyme 1 (*Lyz1*), granzyme M (*Gzmm*), and interferon-induced transmembrane proteins 1, 3, and 6 (*Ifitm1*, *Ifitm3*, and *Ifitm6*). Within the downregulated genes in the *Cebpg* KO NK cells, we identified interferon regulatory factor 2-binding protein (*Irf2pb1*), vascular endothelial growth factor A (*Vegfa*), and IL-15 receptor alpha chain (*Il15rα*).

In parallel, supernatants from the overnight cultures were analyzed by a flow cytometry-based cytokine bead array, which allows identification and quantification of a panel of cytokines. We observed that, upon NK cell activation, IFNγ production was diminished in *Cebpg*-deficient NK cells in comparison with WT NK cells (Figure 6C). Altogether, our findings identified a list of genes and pathways potentially mediating the negative NK cell effects on HSC function, and suggested that IFNγ production by NK cells may negatively affect HSCs during transplantation.

IFNγ-neutralizing antibody restores HSC function in the presence of WT NK cells *in vitro* and *in vivo*

Based on our observations, we first assessed whether IFNγ-neutralizing antibody would rescue the deleterious effect of NK cells on HSCs in culture. We observed that the number of colonies was restored when IFNγ-neutralizing antibody was added to the WT NK-containing cultures, while the presence of IFNγ-neutralizing antibody did not alter colony numbers with or without *Cebpg* KO NK cells (Figure 6D). Since humanized anti-IFNγ monoclonal antibodies are available and ready for clinical use, we next investigated whether inhibition of the IFNγ signaling pathway could improve short-term engraftment, a critical phase during human HSCT. G-CSF mobilized peripheral blood was transplanted into NSG mice, and, 4 h after transplantation, treatment with either IFNγ-blocking antibodies or IgG control was initiated and continued as indicated in Figure 6E. We observed that mice treated with IFNγ-blocking antibodies exhibited improved percentage and absolute numbers of human $CD45^+$ cells in BM compared with mice treated with IgG control antibody (Figure 6F). Further, we observed that animals that received IFNγ-blocking treatment showed increased relative and absolute numbers of human $CD34^+$ cells in the BM (Figure 6G). Together, our data suggest that blocking IFNγ improves HSC function *in vitro* and engraftment during the early phase of HSCT.

DISCUSSION

Cellular crosstalk between distinct cell types occurs in our organism, including hematopoietic cells. Of particular interest is the relationship that HSCs establish with their neighbor cells (Guezguez et al., 2013; Hoggatt et al., 2016; Mirantes et al., 2014; Schuettpelz and Link, 2013; Schurch et al., 2014). During the last years it became evident that this crosstalk not only regulates normal hematopoiesis but also affects the outcome of certain clinical interventions, such as BM transplantation (Crippa and Bernardo, 2018; Russell et al., 2015; Touzot et al., 2015; Triplett et al., 2015). In the present study, we showed that NK cells, an important component of the innate immune system, negatively affect HSC function during transplantation, and that this detrimental effect can be ameliorated by either (1) removing NK cells from the donor graft, or (2) by blocking IFNγ signaling during HSCT. Previously, the role of NK cells in HSCT has largely been addressed, but with a different focus than ours. The majority of reports focused on the ability of donor NK cells to recognize and kill residual tumor cells; mediate innate immune responses to prevent post-transplant infections; facilitate adaptive immune responses mediated by B and T cells; lyse host dendritic cells, thus reducing the risk of GvHD; and contribute to epithelial regeneration (Leung, 2011; Montaldo et al., 2013; Palmer et al., 2013; Parham and McQueen, 2003; Passweg et al., 2004). In contrast to these studies supporting the influence of NK cells from BM grafts on host cells, our data show that donor NK cells can also directly target donor HSCs and affect their reconstitution potential.

C/EBPγ is a transcription factor known to participate in the maturation and function of NK cells (Di Santo, 2006; Kaisho et al., 1999). Recently, we generated a conditional KO mouse model with specific excision of *Cebpg* in hematopoietic cells (Kardosova et al., 2018). Here, we confirmed the previously reported functional defects in *Cebpg* KO NK cells (Kaisho et al., 1999), and used this model to investigate the potential mechanisms of NK-HSC regulation. Our data demonstrate that *Cebpg*-deficient NK cells, which do not harm HSC fitness, produce reduced levels of IFNγ in comparison with WT NK cells. Accordingly, the use of IFNγ-neutralizing antibodies in culture as well as during HSCT improved HSC function. Thus, our results suggest that the INFγ secreted by NK cells contributes to the detrimental

(C) The percentage of human $CD45^+$ donor cells in murine blood, BM, and SP determined 14 weeks after transplantation. Results for two independent experiments using two healthy BM donors (donor 1 and donor 2) are shown. Y axes indicate the percentage of human $CD45^+$ cells in the indicated tissues. Black boxes indicate animals transplanted with IgG-depleted control BM and red boxes indicate animals transplanted with NK-depleted (CD56 depletion) BM. Transplanted cell doses are indicated as dose 1 (0.5×10^6), dose 2 (1×10^6), and dose 3 (2.5×10^6). Data represent mean ± SD from two independent experiments. Two-tailed Student's t test was used to assess statistical significance, p values were not statistically significant.
See also Figure S4.

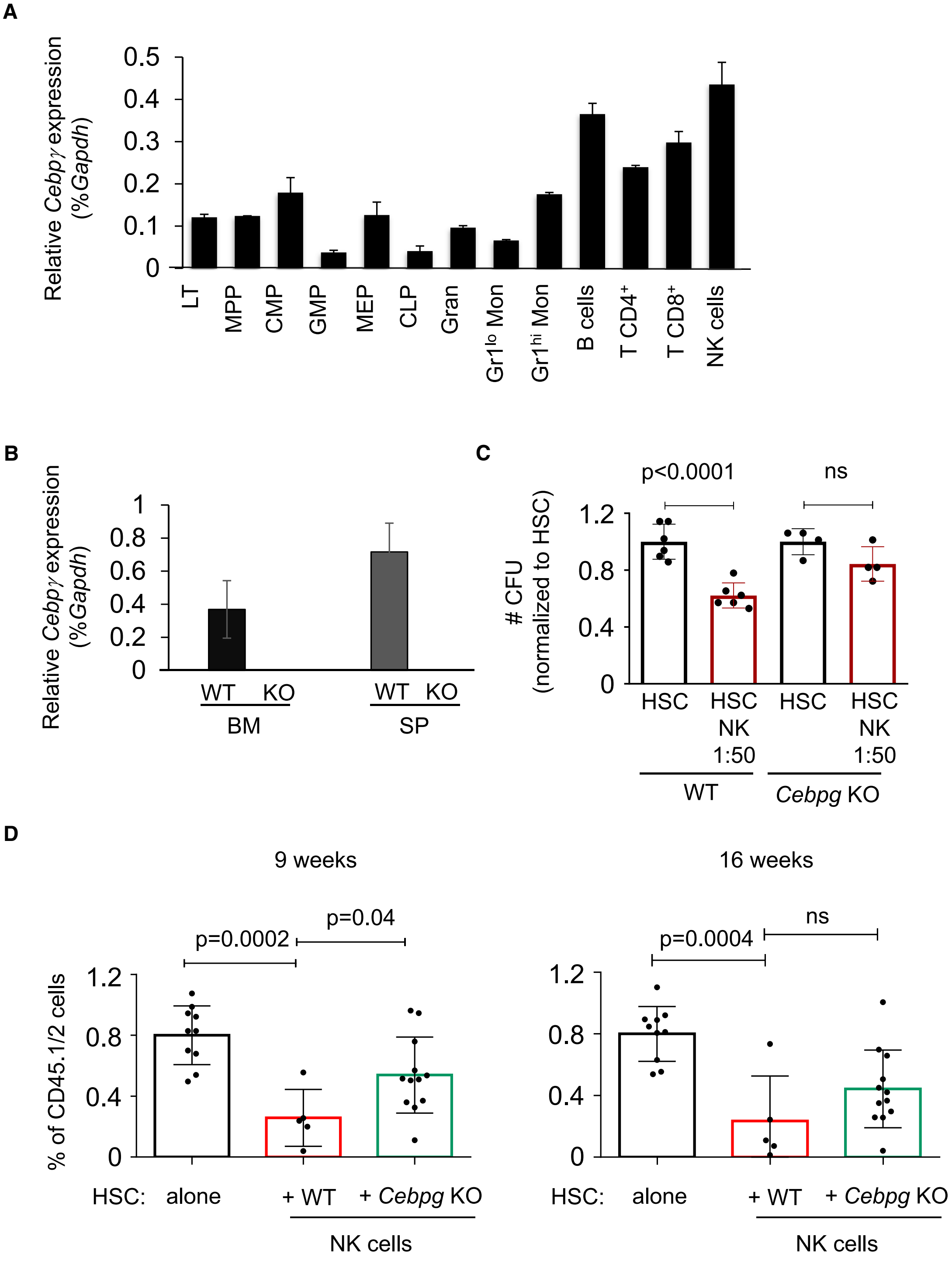

Figure 5. Defective *Cebpg* KO NK cells exhibit milder effects on HSC function than WT NK cells

(A) Relative *Cebpg* expression levels shown as the percentage of *Gapdh* (% *Gapdh*) in distinct sorted hematopoietic cell populations. LT (long-term HSC), MPP (multi-potent progenitor), CMP (common myeloid progenitor), GMP (granulocyte-macrophage progenitor), MEP (megakaryocyte-erythroid progenitor), CLP (common lymphoid progenitor), Gran (granulocyte), $Gr1^{lo}$ Mon ($Gr1^{lo}$ monocyte), $Gr1^{hi}$ Mon ($Gr1^{hi}$ monocyte), B cells, T $CD4^{+}$ cells, T $CD8^{+}$cells, and NK cells.

(B) *Cebpg* mRNA levels in BM and SP isolated from WT and *Cebpg* KO mice. Y axis indicates relative *Cebpg* expression levels relative to *Gapdh* (% *Gapdh*).

(legend continued on next page)

effects on HSC. Accordingly, previous studies suggested negative effects of IFNγ on HSC function. For instance, enhanced proliferation of HSCs and reduction in long-term repopulating capacity was associated with IFNγ stimulation of murine cells in experimental models of bacterial infection (Baldridge et al., 2010; MacNamara et al., 2011). In agreement, Yang et al. (2005) showed that the ability of $CD34^{+}CD38^{-}$ human cord blood cells to support hematopoiesis was inhibited by IFNγ treatment in a xenotransplant model. However, IFNγ is not exclusively produced by NK cells, and other immune cells, such as T cells, can also produce INFγ and, consequently, contribute to the deleterious effects on HSCs. In fact, T cells produce IFNγ and TNFα, and it was recently suggested that neutralizing T cell-mediated TNFα signaling was able to enhance engraftment and hematopoietic reconstitution upon HSCT (Wang et al., 2017). Together, these studies seed the path to potentially novel strategies directed to enhance and improve HSCT, in particular during the critical early stages upon transplantation. Further studies may address whether anti-inflammatory regimes shortly after transplantation, and for a limited period of time, may improve HSCT.

In our assays, since HSCs and mature NK cells were both isolated from the same mouse strain that differed only in CD45.1 or CD45.2 expression (congenic mice), no differential expression of MHC class I ligands was expected. Therefore, we assumed that the observed effects were associated with NK secretory function rather than being dependent on the classic NK missing self-recognition function. Accordingly, gene expression analysis of *Cebpg*-deficient NK cells, compared with controls, revealed deregulation of genes from several cytokine pathways. It was previously reported that, when BM cells were placed under ideal culture conditions, the addition of activated NK cells to the culture inhibited colony formation (Murphy et al., 1992). Our overnight co-cultures followed by frequency and functional assessment indicated reduced HSC numbers and activity in the presence of NK cells, which could be at least partially explained by a reduction in viability. However, these effects were lost when *Cebpg* KO NK cells were employed. Together, based on our observations on the crosstalk between HSCs and NK cells in culture and during HSCT, we hypothesize that the presence of NK cells in the BM microenvironment can modulate HSC activity. However, further studies will need to address whether the co-existence of these cell types in the BM niche during steady-state hematopoiesis may modulate HSC fitness.

It is important to consider that NK cell activity during HSCT may differ depending on the origin of the NK cells (i.e., recipient NK versus donor NK cells). Recipient NK cell subsets bearing MHC class I receptors are said to be licensed or educated, and rapidly respond to stimuli (Alvarez et al., 2016). While licensed recipient NK subsets have been implicated in inhibition of allogenic BM cells and consequent rejection, unlicensed recipient NK cells seem to be growth promoting, thus facilitating BM engraftment (Sun et al., 2012). In the clinical setting, it is undeniable that NK cells play a relevant role in promoting the clearance of malignant cells and avoiding HSCT complications, particularly in HLA-haploidentical transplants (Di Santo, 2006). Here, we describe a novel non-HLA-dependent 'graft NK' - 'graft HSC' regulation mechanism that may influence transplant outcome. The presence of NK cells in the graft, which are also transplanted and activated during the graft product infusion, may harm HSCs contained in the graft regardless of the 'missing self' recognition mechanism, and therefore impair engraftment. It is certainly beneficial to have NK donor cell-rich preparations for malignant diseases such as acute leukemias because of the desired graft-versus-leukemia (GvL) effect. However, we would like to propose that NK cell depletion may actually favor HSC donor engraftment in the setting of allogeneic transplantation for non-neoplastic diseases in selected patients. Such cases would include for instance, but are not limited to, patients with idiopathic severe aplastic anemia or sickle cell anemia. For those situations where GvL effect is not needed, having highly functional donor HSCs may accelerate blood recovery and increase the chances of sustained donor engraftment. NK depletion could gain great value when clinicians deal with limited donor cell numbers. Low number of HSCs in BM preparations can be a problem when insufficient HLA-matched cord blood sources are available for adult patients, such as in geographical regions where mixed ethnicity impairs HLA-matched donor availability. Also, peripheral blood mobilized cells (PBMCs) used for autologous

(C) Colony culture assays of murine cells. Y axis indicates the number of CFU relative to HSC condition. X axis indicates culture conditions: HSC alone or in the presence of WT or *Cebpg* KO NK cells. Cell ratio is indicated. Each dot represents one culture dish. Data represent mean ± SD from three independent experiments.

(D) Engraftment of CD45.1/2 cells in blood of recipient CD45.1 mice evaluated 9 (left) and 16 weeks (right) after transplantation. X axis indicates transplant conditions where purified HSCs alone or with WT or *Cebpg* KO NK cells were co-cultured overnight in the presence IL-2 prior to transplantation. Y axis demonstrates the percentage of CD45.1/2 cells. Each dot indicates values for one animal. All data represent mean ± SD from two independent experiments. For (C) and (D), two-tailed Student's t test was used to assess statistical significance (p values are indicated; ns, not significant).

See also Figure S5.

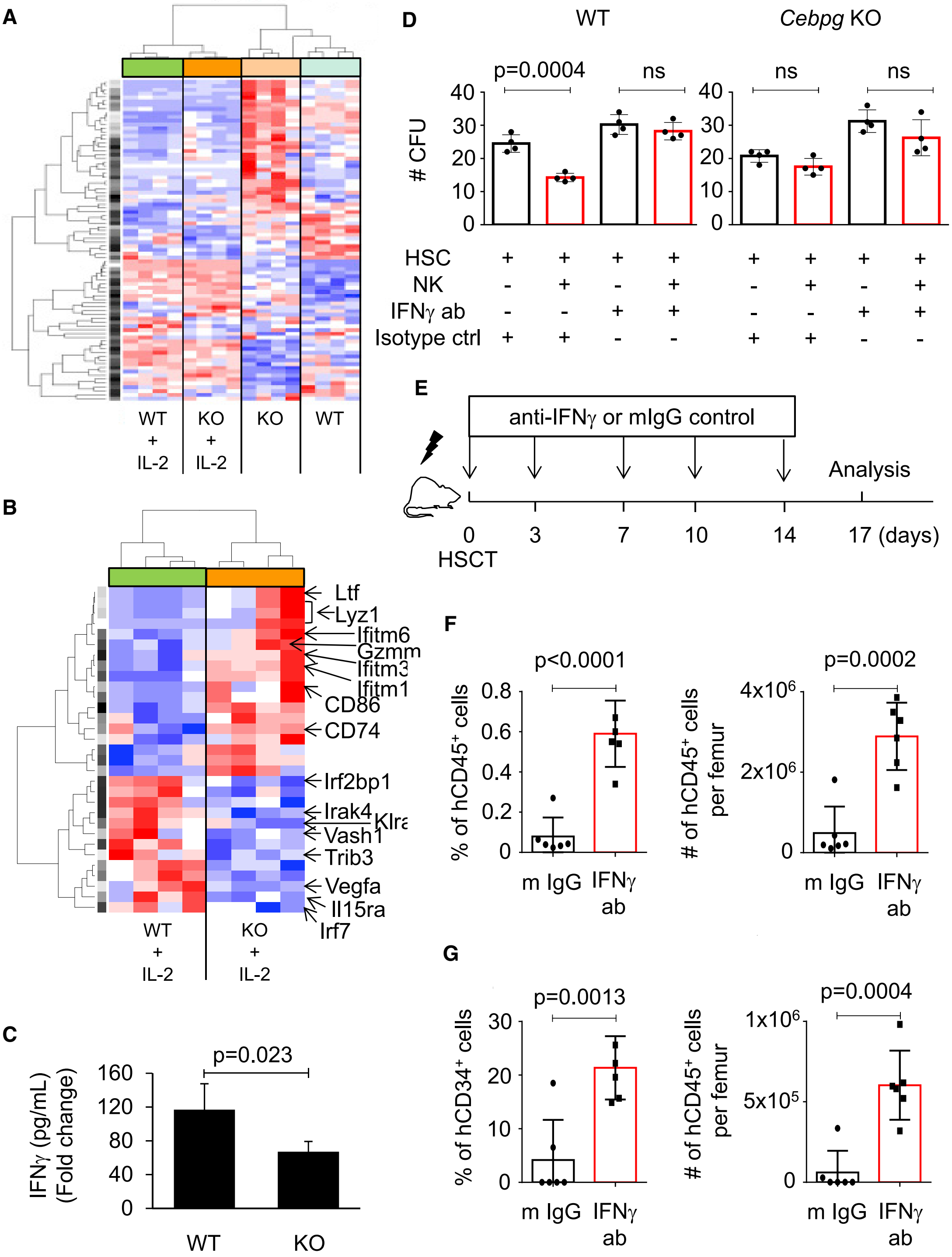

Figure 6. *Cebpg* deletion results in reduced IFNγ production in NK cells and blocking IFNγ signaling improves HSC fitness
(A) Heatmap and hierarchical clustering based on gene expression of 84 probe sets, which compose the NK signature. NK cells were isolated from WT and *Cebpg* KO murine SPs in non-stimulation conditions or upon stimulation with the NK cell-activating cytokine IL-2 (n = 4 for each condition). Data were normalized to z scores for each gene. Red/blue color indicates increase/decrease in gene expression relative to the universal mean for each gene. See also Table S1.

(legend continued on next page)

Table 1. *Cebpg* ablation results in differential pathway enrichment analysis in WT and *Cebpg* KO NK cells stimulated with IL-2

Index	Name	p value	*Z* score	Combined score
1	interferon-gamma signaling pathway	0.01414	−1.57	1.56
2	insulin/IGF pathway-mitogen activated protein kinase kinase/MAP kinase cascade	0.01625	−1.47	1.46
3	apoptosis signaling pathway	0.01821	−1.40	1.39
4	oxidative stress response	0.02026	−0.78	0.77
5	T cell activation	0.02227	−1.20	1.20

Results of Panther pathway analysis of IL-2-treated WT versus *Cepbg* KO NK cells with the threshold of $p < 0.05$.

transplantation in cancer patients undergoing aggressive therapy frequently have low numbers of HSCs.

Future prospective studies are needed to investigate whether NK frequency in HSC donor sources may be proved to be an additional non-HLA risk factor for BM transplantation outcomes together with recipient age, stage of disease, cytomegalovirus (CMV) serostatus, and comorbidities. If this is true, improving HSC function in bone marrow grafts by reducing the effect of NK cells can be clinically important to make BM transplantation feasible for individualized selected patients and to accelerate engraftment in adverse conditions for both allogeneic and autologous transplantation.

EXPERIMENTAL PROCEDURES

Mice

The cell subsets used for this study were obtained from WT C57BL/6 CD45.1, C57BL/6 CD45.2, or C57BL/6 CD45.1/CD45.2 congenic mouse strain. A *Cebpg* conditional KO mouse model was generated by our group and backcrossed into the C57BL/6 background (Kardosova et al., 2018). *Cebpg*$^{flox/flox}$ (*Cebpg*$^{f/f}$) mice were bred to Vav-iCre transgenic mice (also in C57BL/6 background) to generate *Cebpg*$^{f/f}$ Vav-iCre^{-} mice (control, WT) or *Cebpg*$^{f/f}$ Vav-iCre^{+} (KO with *Cebpg* specifically excised in the hematopoietic system), and used for experimental comparisons in this study. Transplantations of human samples were performed on NSG mice (Jackson Laboratory, stock no. 005557), which were maintained in specified pathogen-free conditions. All mice were housed in a sterile barrier facility.

Isolation of murine NK and HSC cells

NK cells were obtained from SP from WT C56BL/6, *Cebpg*$^{f/f}$ Vav-iCre^{-}, and *Cebpg*$^{f/f}$ Vav-iCre^{+} (CD45.2^{+}) mice. HSCs were obtained from WT C57BL/6 CD45.2 or C57BL/6 CD45.1/CD45.2 mice. SP cell suspensions were obtained and submitted to red blood cell (RBC) lysis, followed by immunomagnetic lineage depletion using Ter119, CD4, CD8, and CD19 biotinylated antibodies (BioLegend) and Anti-Biotin Microbeads Ultrapure (Miltenyi Biotec), and then sorted by flow cytometry as lineage negative, CD3 negative, and NK1.1 positive (Lin^{-}, CD3^{-}, NK1.1^{+}). To obtain RNA and cell supernatants, 2.5 × 10^{5} NK cells were cultured in RPMI1640 supplemented with 10% FBS and 1000 U/mL of IL-2 for 24 h. To isolate HSCs, BM samples were lysed by RBC lysis buffer and subsequently depleted using antibodies against Ter-119, CD19, B220, CD8, Gr1, and CD11b antigens by immunomagnetic separation, and then sorted as c-Kit^{hi}, Sca-1^{+}, lineage-negative, CD48^{-}, CD150^{+} cells. Culture conditions are detailed in the online supplemental information.

Flow cytometry

Single-cell suspensions from murine PB, BM, or SP were analyzed by flow cytometry using the following monoclonal antibodies conjugated with biotin (BIO), fluorescein isothiocyanate (FITC), phycoerythrin (PE), PE-Cy5, PE–Cy7, Pacific Blue (PB), allophycocyanin (APC), or APC–Cy7 and obtained from BioLegend or eBioscience: CD19 (MB19-1), B220 (RA3-6B2), CD4 (RM4-5), CD8 (53–6.7), Gr1 (RB6-8C5), CD11b (M1/70), TER119 (TER-119), Sca-1 (D7), streptavidin, c-Kit (2B8), CD48 (HM48-1), CD150 (TC15-12F12.2), CD3 (17A2), NK1.1 (PK136), NKG2A (20d5), NKG2D (CX5), Ly-49H (3D10), CD45.1 (A20), and CD45.2 (104). Stained cells were analyzed with an LSRII flow cytometer and sorted using a FACSAria II or Influx (BD Biosciences).

(B) Heatmap and hierarchical clustering according to expression of 29 genes present in the NK signature. WT and *Cepbg* KO NK cells were treated with IL-2 prior to gene expression profile analysis. Several genes deregulated between the two groups are indicated.
(C) IFNγ levels in supernatants after culturing overnight WT or *Cebpg* KO NK cells. Cultures were established in the absence or presence of IL-2. Y axes indicate cytokine levels (pg/mL) related to the condition without IL-2 for WT and KO NK cells (fold change). n = 4 mice per group, two independent experiments.
(D) Colony culture assays of murine cells. Y axes indicate the number of CFU. X axes indicate culture conditions: NK cells correspond to WT or *Cebpg* KO mice as indicated. Each dot represents one culture well, two independent experiments were performed.
(E) Illustration of the experimental scheme. Arrows and numbers indicate days when treatment was administered. Seventeen days after transplantation, recipient NSG mice were sacrificed and analyzed.
(F and G) Relative percentage (left graphics) and absolute number of cells per femur (right graphics). Y axes indicate the percentage (%) and numbers (#) of human CD45^{+} cells (F) and CD34^{+} cells (G) in BM. Black boxes indicate values for mice that received treatment with mouse IgG control antibodies, and red boxes indicate values for mice that received IFNγ-blocking antibody treatment. Each animal is indicated by a symbol (n = 5–6 animals per group). For (C), (D), (F) and (G), data represent mean ± SD, two-tailed Student's t test was used to assess statistical significance (p values are indicated; ns, not significant).

Viable cells were identified by Hoechst 33258 exclusion. Diva (BD Biosciences) and FlowJo (Tree Star) software were used for data acquisition and analysis, respectively. CountBright Absolute Counting Beads (Molecular probes, Invitrogen) were used for HSC subpopulation quantification by flow cytometry.

Study approval

Animal studies were approved by the Institutional Animal Care and Use Committee (IACUC) at the Beth Israel Deaconess Medical Center (Boston, United States) and by the Animal Ethical Committee at the Institute of Molecular Genetics (Prague, Czech Republic). Human BM samples were obtained after written informed consent was received from participants. Human studies were approved by the institutional review board at the First Faculty of Medicine, Charles University in Prague and General University Hospital (Prague, Czech Republic).

Statistical analysis

Statistical significance for indicated datasets was determined using two-sided, unpaired Student's t test, and p values < 0.05 were considered statistically significant. Scatter dot plots depict mean with error bars representing standard deviation (SD). Jonckheere-Terpstra trend tests (for group comparisons) using the SPSS software version 20 was employed when indicated. HSC frequencies were calculated with L-Calc software (StemCell Technologies, Vancouver, Canada) using Poisson statistics and the method of maximum likelihood to the proportion of negative recipients in a limiting dilution setting.

Data and code availability

The accession number for the microarray data reported in this paper is ArrayExpress: E-MTAB-5604.

SUPPLEMENTAL INFORMATION

Supplemental information can be found online at https://doi.org/10.1016/j.stemcr.2021.06.008.

AUTHOR CONTRIBUTIONS

Conceptualization, L.L.d.F-P., R.S.W., D.G.T., and M.A.-J.; methodology, L.L.d.F-P., R.S.W, S.L., and M.A.-J.; formal analysis, L.L.d.F-P., H.S., and M.A.-J.; investigation, L.L.d.F-P., R.S.W, M.K.A., S.G., M.K., I.A.L., A.F.d.O.C., H.Z., A.M., A.T.J., M.Z., and M.A.-J.; data curation, H.S.; writing, L.L.d.F-P. and M.A.-J.; visualization, L.L.d.F-P. and M.A.-J.; supervision, L.L.d.F-P., R.S.W., D.G.T., and M.A.-J.; funding acquisition, L.L.d.F-P., D.G.T., and M.A.-J.

DECLARATION OF INTERESTS

The authors declare no competing interests.

ACKNOWLEDGMENTS

This work was supported by a grant from São Paulo Research Foundation (FAPESP; grant 2015/21866-1) to L.L.d.F.-P. M.A.-J. was supported by a GACR grant 18-08577S and institutional funding from the IMG CAS (RVO 68378050). D.G.T. was supported by a STaR Investigator Award, an RCE Core grant, and Tier 3 RNA Biology Center grant MOE2014-T3-1-006 from the NRF and MOE, Singapore, and NIH grants R35CA197697 and P01HL131477. The authors thank Prof. Vaclav Horejsi for providing us with the IFNγ and IgG1 antibodies.

Received: October 24, 2019
Revised: June 10, 2021
Accepted: June 10, 2021
Published: July 8, 2021

REFERENCES

Alvarez, M., Sun, K., and Murphy, W.J. (2016). Mouse host unlicensed NK cells promote donor allogeneic bone marrow engraftment. Blood *127*, 1202–1205.

Baldridge, M.T., King, K.Y., Boles, N.C., Weksberg, D.C., and Goodell, M.A. (2010). Quiescent haematopoietic stem cells are activated by IFN-gamma in response to chronic infection. Nature *465*, 793–797.

Buza-Vidas, N., Antonchuk, J., Qian, H., Mansson, R., Luc, S., Zandi, S., Anderson, K., Takaki, S., Nygren, J.M., Jensen, C.T., et al. (2006). Cytokines regulate postnatal hematopoietic stem cell expansion: opposing roles of thrombopoietin and LNK. Genes Dev. *20*, 2018–2023.

Chen, C., Busson, M., Rocha, V., Appert, M.L., Lepage, V., Dulphy, N., Haas, P., Socie, G., Toubert, A., Charron, D., et al. (2006). Activating KIR genes are associated with CMV reactivation and survival after non-T-cell depleted HLA-identical sibling bone marrow transplantation for malignant disorders. Bone Marrow Transplant. *38*, 437–444.

Crippa, S., and Bernardo, M.E. (2018). Mesenchymal stromal cells: role in the BM niche and in the support of hematopoietic stem cell transplantation. Hemasphere *2*, e151.

Di Santo, J.P. (2006). Natural killer cell developmental pathways: a question of balance. Annu. Rev. Immunol. *24*, 257–286.

Geerman, S., Brasser, G., Bhushal, S., Salerno, F., Kragten, N.A., Hoogenboezem, M., de Haan, G., Wolkers, M.C., Pascutti, M.F., and Nolte, M.A. (2018). Memory CD8(+) T cells support the maintenance of hematopoietic stem cells in the bone marrow. Haematologica *103*, e230–e233.

Geerman, S., and Nolte, M.A. (2017). Impact of T cells on hematopoietic stem and progenitor cell function: good guys or bad guys? World J. Stem Cells *9*, 37–44.

Guezguez, B., Campbell, C.J., Boyd, A.L., Karanu, F., Casado, F.L., Di Cresce, C., Collins, T.J., Shapovalova, Z., Xenocostas, A., and Bhatia, M. (2013). Regional localization within the bone marrow influences the functional capacity of human HSCs. Cell Stem Cell *13*, 175–189.

Hirata, Y., Furuhashi, K., Ishii, H., Li, H.W., Pinho, S., Ding, L., Robson, S.C., Frenette, P.S., and Fujisaki, J. (2018). CD150(high) bone marrow Tregs maintain hematopoietic stem cell quiescence and immune privilege via adenosine. Cell Stem Cell *22*, 445–453.

Hoggatt, J., Kfoury, Y., and Scadden, D.T. (2016). Hematopoietic stem cell niche in health and disease. Annu. Rev. Pathol. *11*, 555–581.

Joncker, N.T., Shifrin, N., Delebecque, F., and Raulet, D.H. (2010). Mature natural killer cells reset their responsiveness when exposed to an altered MHC environment. J. Exp. Med. *207*, 2065–2072.

Kaisho, T., Tsutsui, H., Tanaka, T., Tsujimura, T., Takeda, K., Kawai, T., Yoshida, N., Nakanishi, K., and Akira, S. (1999). Impairment of natural killer cytotoxic activity and interferon gamma production in CCAAT/enhancer binding protein gamma-deficient mice. J. Exp. Med. *190*, 1573–1582.

Kardosova, M., Zjablovskaja, P., Danek, P., Angelisova, P., de Figueiredo-Pontes, L.L., Welner, R.S., Brdicka, T., Lee, S., Tenen, D.G., and Alberich-Jorda, M. (2018). C/EBPgamma is dispensable for steady-state and emergency granulopoiesis. Haematologica *103*, e331–e335.

Kim, S., Poursine-Laurent, J., Truscott, S.M., Lybarger, L., Song, Y.J., Yang, L., French, A.R., Sunwoo, J.B., Lemieux, S., Hansen, T.H., et al. (2005). Licensing of natural killer cells by host major histocompatibility complex class I molecules. Nature *436*, 709–713.

Leung, W. (2011). Use of NK cell activity in cure by transplant. Br. J. Haematol. *155*, 14–29.

MacNamara, K.C., Jones, M., Martin, O., and Winslow, G.M. (2011). Transient activation of hematopoietic stem and progenitor cells by IFNgamma during acute bacterial infection. PLoS one *6*, e28669.

Mehta, R.S., Shpall, E.J., and Rezvani, K. (2015). Cord blood as a source of natural killer cells. Front. Med. *2*, 93.

Mirantes, C., Passegue, E., and Pietras, E.M. (2014). Pro-inflammatory cytokines: emerging players regulating HSC function in normal and diseased hematopoiesis. Exp. Cel. Res. *329*, 248–254.

Montaldo, E., Vacca, P., Moretta, L., and Mingari, M.C. (2013). Understanding human NK cell differentiation: clues for improving the haploidentical hematopoietic stem cell transplantation. Immunol. Lett. *155*, 2–5.

Murphy, W.J., Keller, J.R., Harrison, C.L., Young, H.A., and Longo, D.L. (1992). Interleukin-2-activated natural killer cells can support hematopoiesis in vitro and promote marrow engraftment in vivo. Blood *80*, 670–677.

Palmer, J.M., Rajasekaran, K., Thakar, M.S., and Malarkannan, S. (2013). Clinical relevance of natural killer cells following hematopoietic stem cell transplantation. J. Cancer *4*, 25–35.

Parham, P., and McQueen, K.L. (2003). Alloreactive killer cells: hindrance and help for haematopoietic transplants. Nat. Rev. Immunol. *3*, 108–122.

Passweg, J.R., Tichelli, A., Meyer-Monard, S., Heim, D., Stern, M., Kuhne, T., Favre, G., and Gratwohl, A. (2004). Purified donor NK-lymphocyte infusion to consolidate engraftment after haploidentical stem cell transplantation. Leukemia *18*, 1835–1838.

Raziuddin, A., Longo, D.L., Bennett, M., Winkler-Pickett, R., Ortaldo, J.R., and Murphy, W.J. (2002). Increased bone marrow allograft rejection by depletion of NK cells expressing inhibitory Ly49 NK receptors for donor class I antigens. Blood *100*, 3026–3033.

Ruggeri, L., Capanni, M., Urbani, E., Perruccio, K., Shlomchik, W.D., Tosti, A., Posati, S., Rogaia, D., Frassoni, F., Aversa, F., et al. (2002). Effectiveness of donor natural killer cell alloreactivity in mismatched hematopoietic transplants. Science *295*, 2097–2100.

Russell, A., Malik, S., Litzow, M., Gastineau, D., Roy, V., and Zubair, A.C. (2015). Dual roles of autologous CD8+ T cells in hematopoietic progenitor cell mobilization and engraftment. Transfusion *55*, 1758–1765, quiz 1757.

Schuettpelz, L.G., and Link, D.C. (2013). Regulation of hematopoietic stem cell activity by inflammation. Front. Immunol. *4*, 204.

Schurch, C.M., Riether, C., and Ochsenbein, A.F. (2014). Cytotoxic CD8+ T cells stimulate hematopoietic progenitors by promoting cytokine release from bone marrow mesenchymal stromal cells. Cell Stem Cell *14*, 460–472.

Storek, J., Gooley, T., Witherspoon, R.P., Sullivan, K.M., and Storb, R. (1997). Infectious morbidity in long-term survivors of allogeneic marrow transplantation is associated with low CD4 T cell counts. Am. J. Hematol. *54*, 131–138.

Sun, K., Alvarez, M., Ames, E., Barao, I., Chen, M., Longo, D.L., Redelman, D., and Murphy, W.J. (2012). Mouse NK cell-mediated rejection of bone marrow allografts exhibits patterns consistent with Ly49 subset licensing. Blood *119*, 1590–1598.

Tomblyn, M., Young, J.A., Haagenson, M.D., Klein, J.P., Trachtenberg, E.A., Storek, J., Spellman, S.R., Cooley, S., Miller, J.S., and Weisdorf, D.J. (2010). Decreased infections in recipients of unrelated donor hematopoietic cell transplantation from donors with an activating KIR genotype. Biol. Blood Marrow Transplant. *16*, 1155–1161.

Touzot, F., Neven, B., Dal-Cortivo, L., Gabrion, A., Moshous, D., Cros, G., Chomton, M., Luby, J.M., Terniaux, B., Magalon, J., et al. (2015). CD45RA depletion in HLA-mismatched allogeneic hematopoietic stem cell transplantation for primary combined immunodeficiency: a preliminary study. J. Allergy Clin. Immunol. *135*, 1303–1309 e1301.

Triplett, B.M., Shook, D.R., Eldridge, P., Li, Y., Kang, G., Dallas, M., Hartford, C., Srinivasan, A., Chan, W.K., Suwannasaen, D., et al. (2015). Rapid memory T-cell reconstitution recapitulating CD45RA-depleted haploidentical transplant graft content in patients with hematologic malignancies. Bone Marrow Transplant. *50*, 1012.

Venstrom, J.M., Gooley, T.A., Spellman, S., Pring, J., Malkki, M., Dupont, B., Petersdorf, E., and Hsu, K.C. (2010). Donor activating KIR3DS1 is associated with decreased acute GVHD in unrelated allogeneic hematopoietic stem cell transplantation. Blood *115*, 3162–3165.

Vivier, E., Tomasello, E., Baratin, M., Walzer, T., and Ugolini, S. (2008). Functions of natural killer cells. Nat. Immunol. *9*, 503–510.

Wagner, J.E., Thompson, J.S., Carter, S.L., and Kernan, N.A. (2005). Effect of graft-versus-host disease prophylaxis on 3-year disease-free survival in recipients of unrelated donor bone marrow (T-cell Depletion Trial): a multi-centre, randomised phase II-III trial. Lancet *366*, 733–741.

Wang, W., Fujii, H., Kim, H.J., Hermans, K., Usenko, T., Xie, S., Luo, Z.J., Ma, J., Celso, C.L., Dick, J.E., et al. (2017). Enhanced human hematopoietic stem and progenitor cell engraftment by blocking donor T cell-mediated TNFalpha signaling. Sci. Transl. Med. *9*, eaag3214.

Yang, L., Dybedal, I., Bryder, D., Nilsson, L., Sitnicka, E., Sasaki, Y., and Jacobsen, S.E. (2005). IFN-gamma negatively modulates self-renewal of repopulating human hemopoietic stem cells. J. Immunol. *174*, 752–757.

Zhang, C.C., and Lodish, H.F. (2008). Cytokines regulating hematopoietic stem cell function. Curr. Opin. Hematol. *15*, 307–311.

Stem Cell Reports, Volume *16*

Supplemental Information

Improved hematopoietic stem cell transplantation upon inhibition of natural killer cell-derived interferon-gamma

Lorena Lobo de Figueiredo-Pontes, Miroslava K. Adamcova, Srdjan Grusanovic, Maria Kuzmina, Izabela Aparecida Lopes, Amanda Fernandes de Oliveira Costa, Hong Zhang, Hynek Strnad, Sanghoon Lee, Alena Moudra, Anna T. Jonasova, Michal Zidka, Robert S. Welner, Daniel G. Tenen, and Meritxell Alberich-Jorda

Supplemental Table of Contents

Supplemental Experimental Procedures

Supplemental References

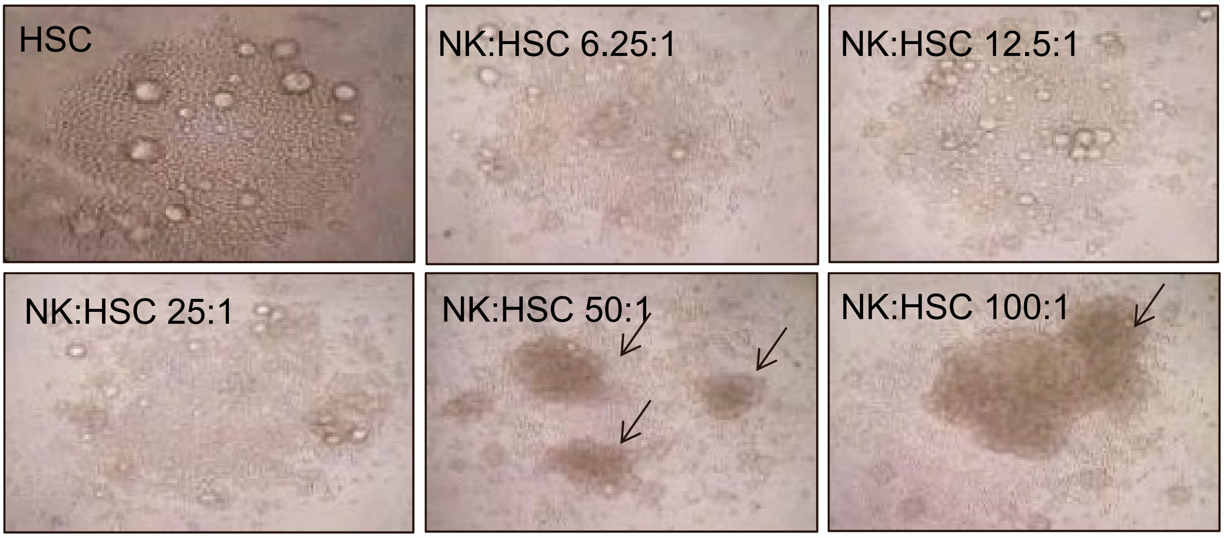

Figure S1. NK cells reduce HSC maintenance and frequency in culture. Related to figure 1. Images of HSC:NK 4-day co-cultures in the presence of IL-2. Pictures were taken by microscopy of the tissue culture plates (100 X). HSC:NK cell ratio is indicated. Arrows indicate non-viable colonies. Notice the reduction in colonies with increasing amounts of NK cells in culture.

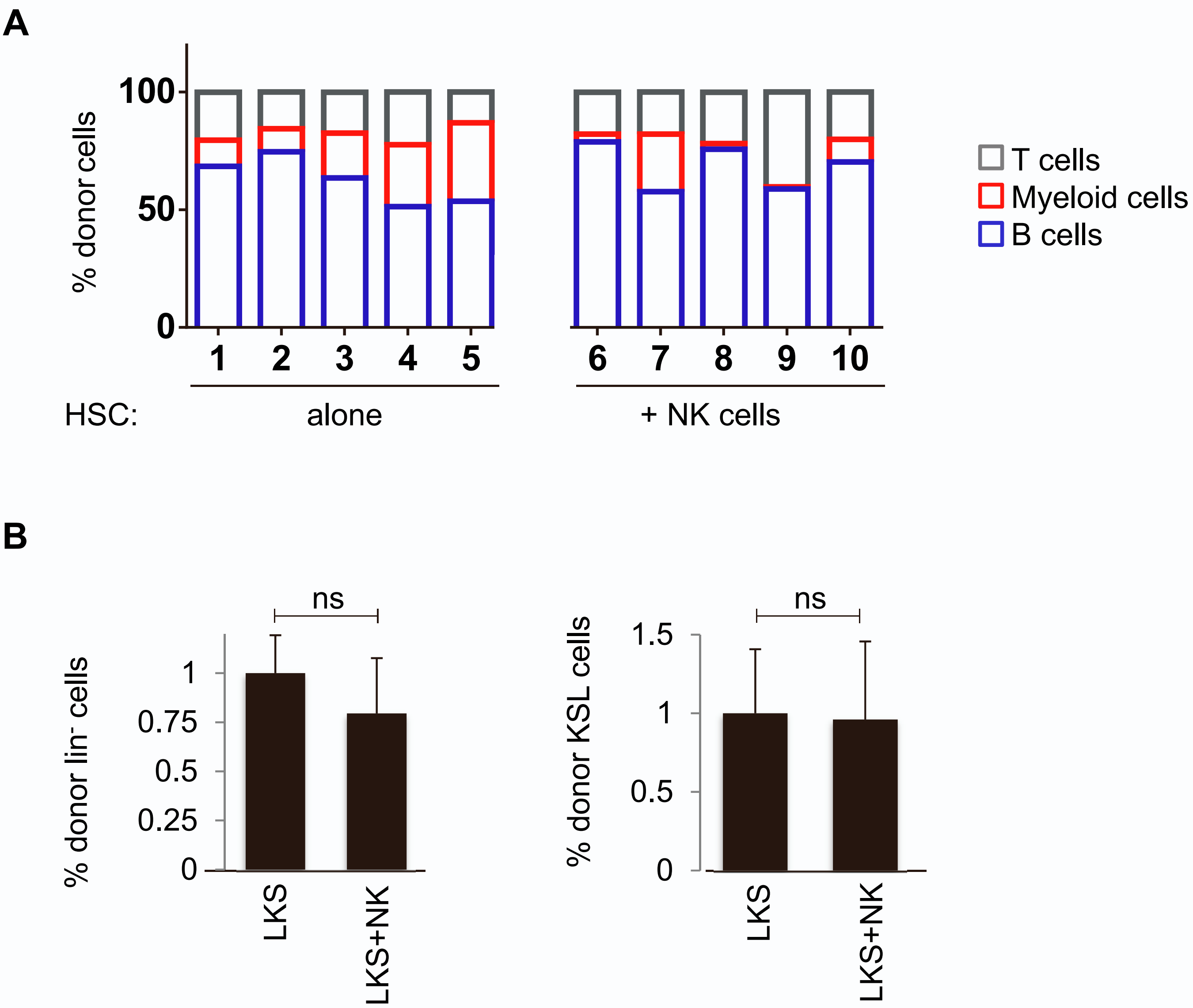

Figure S2. Donor cell contribution to production of T,- B-, myeloid cells and homing assays. Related to figure 2. (A) Blood sample analysis nine weeks post-transplantation. The bars show the average percentages of donor CD45.1/2 cells expressing myeloid (Gr-1 and CD11b), B- (B220), or T- (CD4/8) cell lineage markers. 1-5 indicates mice transplanted with HSC, and 6-10 indicates mice transplanted with HSC exposed to NK cells. (B) Lineage$^-$ c-Kit$^+$ Sca-1$^+$ (LKS) cells (CD45.1) were injected into sublethally irradiated CD45.1/2 mice (n=4 per group) in the presence or absence of NK cells (CD45.2). Bone marrow was obtained from recipients 30 hours after transplant and the percentage of both CD45.1/2 lineage negative cells and LKS cells was measured by flow cytometry analysis. The addition of NK cells to the donor cell preparations did not affect homing of progenitor cells, lineage negative as well as LKS donor cells were quantified, Two-tailed Student's t-test was used to assess statistical significance, ns: not significant ($p \geq 0.05$). Results are shown by normalization of the percentages of recovered cells in the LKS$^+$ NK group to the LKS injected group.

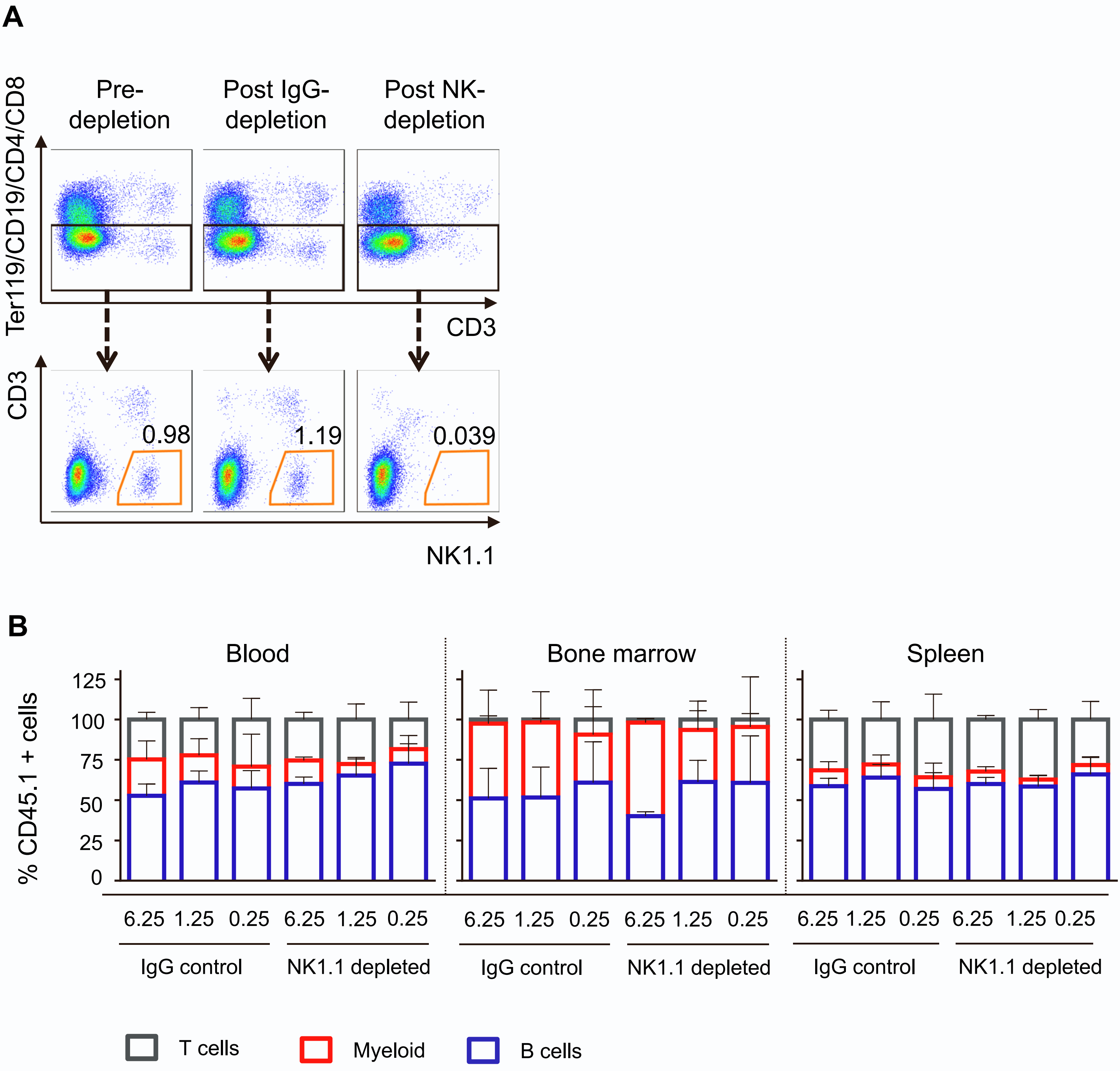

Figure S3. NK cell depletion from murine BM grafts improves hematopoietic recovery of recipient mice. Related to figure 3. (A) Flow cytometry analysis of BM donor samples prior to depletion (pre-depletion), IgG control depleted (post IgG-depletion), and NK cell depleted (post NK-depletion). Upper dot plots indicate Ter119/CD19/CD4/CD8 staining versus CD3 staining. Black box indicates gating used for further analysis shown in lower panels. Lower dot plots show CD3 and NK1.1 staining. Orange box indicates percentage of NK cells ($CD3^{-}NK1.1^{+}$) from alive cells. (B) Lineage contribution of $CD45.1^{+}$ donor cells to blood formation in recipient mice. Y axes indicate the percentage of $CD45.1^{+}$ cells to each lineage. X axes indicate the different groups based on IgG control and NK1.1 depletion. Cell doses used for transplantation are indicated as 6.25 (6.25 x 10^6 cells), 1.25 (1.25 x 10^6 cells) and 0.25 (0.25 x 10^6 cells). Gray boxes indicate the percentage of T cells, red boxes the percentage of myeloid cells, and blue boxes the percentage of B cells. Each column represents average values and standard deviation for at least 5 mice/group.

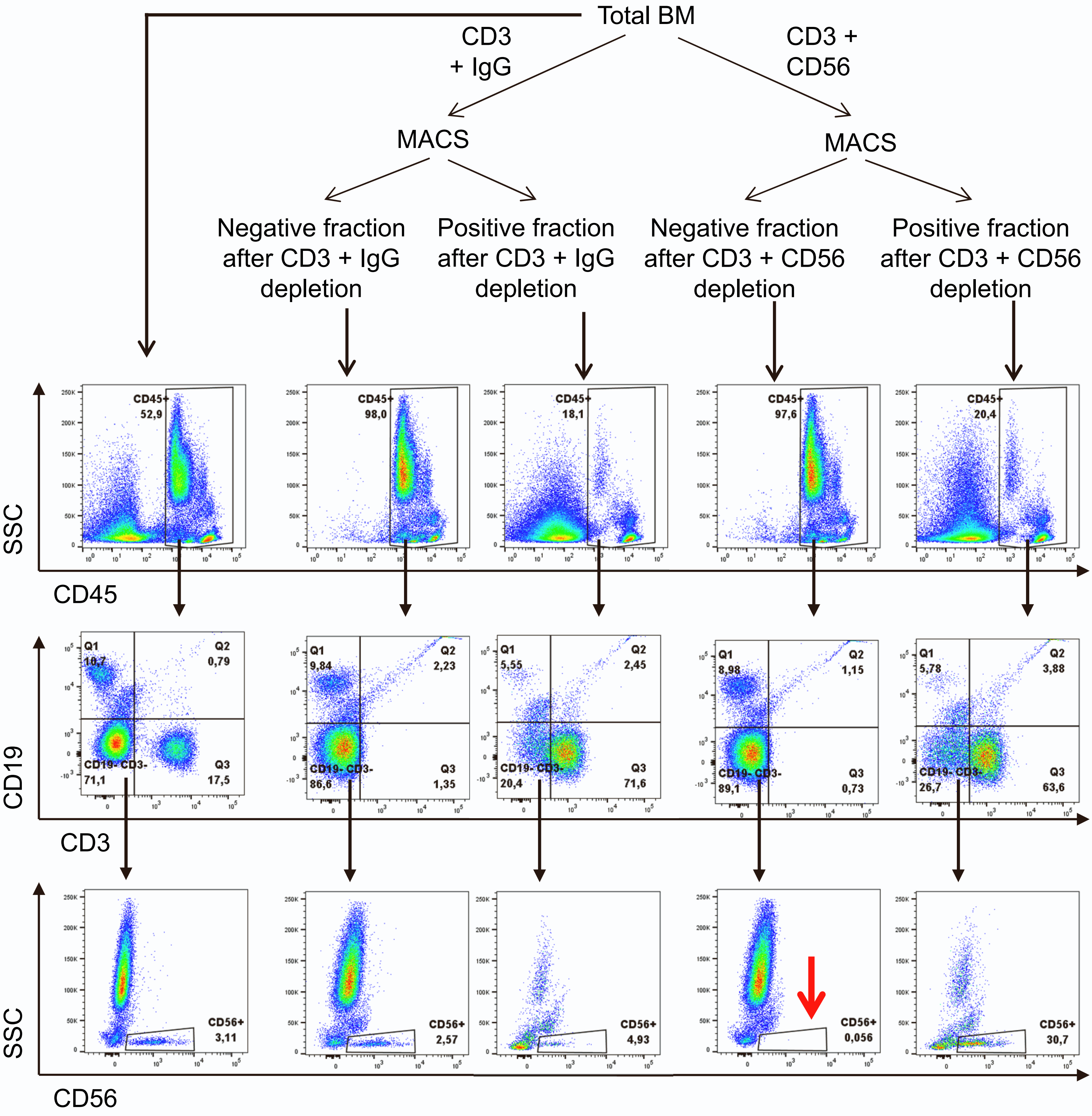

Figure S4. Human bone marrow fractionation. Related to figure 4. Upper scheme: graphical representation of the procedure. BM cells were fractionated based on CD3 and IgG expression or CD3 and CD56 expression. After MACS separation negative and positive fractions were recovered. Lower flow cytometric plots: Separated BM populations were stained using antibodies against CD45, CD19, CD3, and CD56. Red arrow points to the efficiently deleted NK cells.

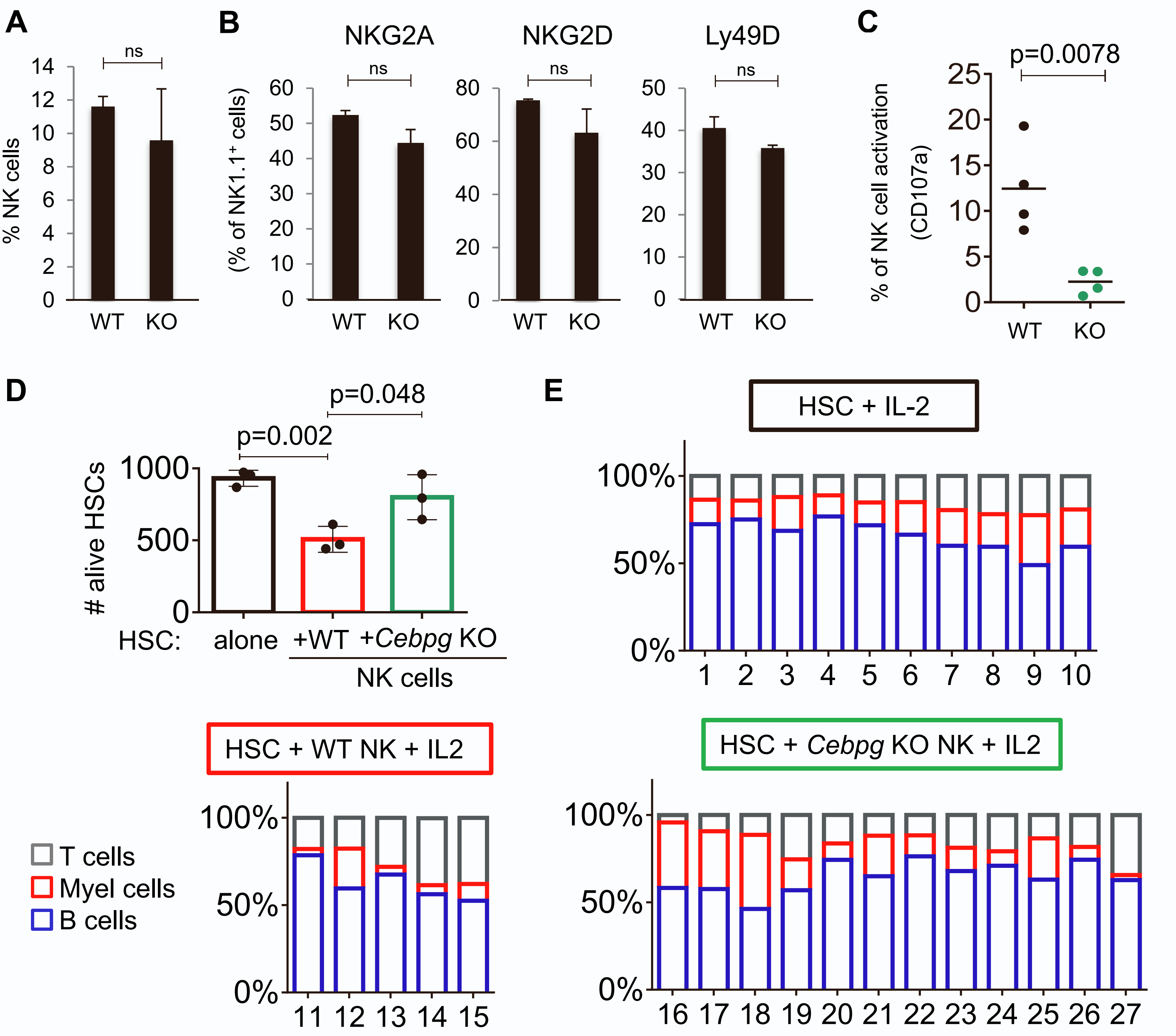

Figure S5. Characterization and function of *Cebpg* KO NK cells in comparison to WT NK cells. Related to figure 5. (A) Percentage of NK cells determined by flow cytometry analysis in WT and *Cebpg* KO spleen cells. NK cells were determined by expression of NK1.1 antigen in the absence of Ter119, CD4, CD8, CD19 and CD3. (B) Expression of the receptors NKG2A, NKG2D and Ly49H in WT and *Cebpg* KO NK cells determined by flow cytometry (n=4 per group). Y axes indicate the expression of each receptor among NK1.1$^+$ gated cells. (C) NK cell cytotoxicity against the murine YAC-1 MHC-I-deficient lymphoma cell line determined by the detection of CD107a by flow cytometry after five hours of a 10:1 ratio of NK:YAC-1 co-culture. Y axis illustrates the percentage (%) of CD107a among NK1.1$^+$ gated cells. (D) Number of HSCs assessed by FACS. Y axis indicates number of alive Hoescht 33258$^-$ HSCs after overnight incubation. X axis indicates culture conditions. (E) Flow cytometry analysis of peripheral blood samples from recipient mice 16 weeks post-transplant. Donor CD45.1/2 cells were analyzed for expression of T (CD3, grey box), myeloid (Gr-1 and CD11b, red box) or B (B220, blue box) cell lineage markers. Y axes indicates percentage of the distinct populations. X axes indicate individual animals: 1-10 transplanted with HSC alone, 11-15 transplanted with HSC co-cultured with WT NK cells, 16-27 transplanted with HSC co-cultured with *Cepbg* KO NK cells, all co-cultures were kept in media with IL-2. Two-tailed Student's t-test was used to assess statistical significance (p values are indicated, ns: not significant).

TABLE S1. List of genes belonging to the NK cell signature. Related to Figure 6.

TABLE S2. Differential pathway enrichment analysis in WT and *Cebpg* KO NK cells. Related to Figure 6.

Index	Name	P-value	Z-score	Combined Score
1	toll like receptor signaling pathway	0.002136	-1.90	3.08
2	apoptosis	0.003123	-1.85	3.00
3	b cell receptor signaling pathway	0.003992	-1.75	2.84
4	vegf signaling pathway	0.01860	-1.82	1.05
5	aminoacyl trna biosynthesis	0.02612	-1.55	0.89
6	pancreatic cancer	0.02696	-1.69	0.97
7	ubiquitin mediated proteolysis	0.02886	-1.28	0.73
8	chronic myeloid leukemia	0.03096	-1.61	0.93
9	c21 steroid hormone metabolism	0.03397	0.75	-0.43
10	cytokine cytokine receptor interaction	0.04043	-1.53	0.87
11	MAPK signaling pathway	0,04184	-1.54	0,87

Results of KEGG pathway analysis of WT versus *Cebpg* KO NK cells with the threshold of $p<0.05$.

SUPPLEMENTAL EXPERIMENTAL PROCEDURES

Co-cultures with OP9 stromal cells

Co-cultures of HSCs (lin$^-$ c-Kit$^+$ Sca-1$^+$ CD48$^-$ CD150$^+$) and NK cells (Ter 119$^-$ CD19$^-$ CD8$^-$ CD4$^-$ CD3$^-$ NK1.1$^+$) in different ratios were performed using serum-free stem cell medium and cytokines (100 ng/mL SCF, 100 ng/mL FLT3-ligand, 10 ng/mL IL-3, 10 ng/mL IL-6, 25 ng/mL TPO, murine IL-2 1000 U/mL) over a confluent layer of mitomycin C treated OP9 stromal cells. 4 days after culture cells were stained for HSC markers (lin$^-$ c-Kit$^+$ Sca-1$^+$ CD48$^-$ CD150$^+$), enumerated by flow cytometry analysis, and colonies were visualized by microscopy.

Murine colony-forming unit (CFU) assays

Co-cultures of HSCs and NK cells were performed using StemSpan serum-free stem cell medium and cytokines (100 ng/mL SCF, 100 ng/mL FLT3-ligand, 10 ng/mL IL-3, 10 ng/mL IL-6, 25 ng/mL TPO, IL-2 1000 U/mL) in 96-well round bottom plates overnight. When indicated, aforementioned media was supplemented with 10 ug/mL neutralizing anti-IFN gamma monoclonal Antibody (clone XMG1.2, eBioscience) or Rat IgG1 kappa Isotype Control (eBRG1, eBioscience). After overnight incubation, cells were plated in methylcellulose-based medium MethoCult GF M3434 (Stemcell Technologies) supplemented with murine IL-2 1000 U/mL. 100 murine HSCs alone or 100 HSCs co-cultured with 1000 or 5000 NK cells were plated in duplicates in 12-well plate. Number of colonies was assessed 10 days after plating.

Human CFU assays

Human CD34$^+$ cells and NK cells (CD19$^-$ CD8$^-$ CD4$^-$ CD3$^-$ CD56$^+$) were isolated from adult bone marrow (BM) obtained from femoral heads removed during hip replacement surgeries. First, mononuclear cells were separated by density gradient centrifugation using Ficoll-Paque PREMIUM (GE Healthcare). One part of the mononuclear cell suspension was frozen and later human NK cells were sorted from thawed material by using BD FACSAriaIIu. Another part was immediately used to obtain CD34$^+$ cells by magnetic separation using human CD34$^+$ MicroBead kit (Miltenyi Biotec) and autoMACS Separator (Miltenyi Biotec). CD34$^+$ cells were frozen as well. Thawed human CD34$^+$ cells were cultured alone or with NK cells from the same patient (ratio 1:10) in serum-free stem cell medium and human cytokines (100 ng/mL SCF, 50 ng/mL G-CSF, 100 ng/mL FLT3-ligand, 25 ng/mL IL-3, 20 ng/mL TPO, IL-2 1000 U/mL) in 96-well round bottom plate overnight. After overnight incubation, cell suspensions of 500 or 1000 CD34$^+$ cells alone or co-cultured with 5000 or 10000 NK cells, respectively, were plated in duplicates in 12-well plate and number of colonies was assessed 10 days after plating. CFU assays were performed using MethoCult H4535 (Stemcell Technologies) supplemented with human IL-2 1000 U/mL (Gibco).

Gene expression analysis

Total RNA was isolated from NK cells sorted from WT and *Cebpg* KO murine spleens cultured in RPMI with 10% FBS overnight in the presence of 1000 U/ml IL-2 (PeproTech) or vehicle. RNA extraction was performed using RNeasy Plus Mini Kit (Qiagen). RNA integrity was analyzed by Agilent Bioanalyzer 2100 (Agilent), and only samples with intact RNA profiles were used for expression profiling (RIN > 7). Four biological replicates were used for each phenotype and treatment. 600 pg RNA was amplified with PicoSL WTASystem V2 (NuGEN), labeled with Encore Biotin IL Module (NuGEN) and 750 ng of labeled RNA was hybridized on MouseRef-8 v2.0 Expression BeadChip (Illumina) according to the manufacturer procedure. Raw data were processed using the beadarray package of Bioconductor and analyzed as described previously(Melenovsky et al., 2011). Gene set enrichment analysis (GSEA) was performed using the Enrichr gene analysis tool (http://amp.pharm.mssm.edu/Enrichr)(Chen et al., 2013). Microarray data were deposited in ArrayExpress (http://www.ebi.ac.uk/arrayexpress) under accession number E-MTAB-5604.

Cytokine assay

A total of 250.000 WT or *Cebpg* KO purified NK cells were cultured in RPMI1640 supplemented with 10% FBS and 1000 U/mL of IL-2 for 24 hours. Then, supernatants were collected, and IL2, IL4, IL6, IL10, IL17A, TNFα and IFNγ cytokine levels were measured by flow cytometry analysis using Cytometric Bead Array technology (BD Biosciences) according to manufacturer's instructions.

Murine BM transplantation

1500 HSCs, defined as lin$^-$ c-Kit$^+$ Sca-1$^+$ CD48$^-$ CD150$^+$ cells, were sorted from mice (CD45.1/2) and cultured with or without IL-2 and/or NK cells (CD3$^-$ NK1.1$^+$) in a ratio of 10^5 NK cells to 1.5×10^3 HSCs per mouse. The 100:1.5 NK:HSC ratio was chosen to roughly mimic the proportions of these two cell subtypes in a normal BM (approximately 1% of NK cells and 0.01% of HSCs). Then, the content of individual wells was mixed together with 0.5×10^6 BM cells as a support (CD45.1) and injected through the tail vein into lethally irradiated (6 Gy)

CD45.1 recipients (3 independent experiments were performed) For engraftment analysis, cells were stained with anti-CD45.1 and CD45.2 antibodies to distinguish donor-derived cells from the host cells, as well as with lineage-specific antibodies Mac1, Gr1, B220 and CD3 to identify myeloid, B and T lineages, respectively. Engraftment analysis was performed after 9 and 16 weeks of transplant.

For murine limiting dilution assays, total BM cells (CD45.1) were submitted to NK1.1 or IgG depletion and then different numbers injected into lethally irradiated (6 Gy) CD45.2 recipients (n=6 or 11 per group, 2 experiments). Peripheral blood was collected from each mouse at 8 and 16 weeks, and BM and spleen were obtained at 16 weeks for final chimerism analysis. For this assay, a recipient mouse was considered positive if >0.1% CD45.1$^+$ cells were detected and three lineages were reconstituted (>1% of CD3$^+$, Gr1$^+$Mac1$^+$ or B220$^+$ cells from CD45.1$^+$ cell population).

NK depletion from murine and human BM

After red blood cells lyse, cells from murine whole BM were stained with 0.1 µg per 10^6 cells (in a 1:50 dilution) of anti-mouse IgG2a (MOPC-173) or NK1.1 (PK136) biotinylated antibodies (Biolegend) for 30 minutes, washed and stained with anti-biotin Microbeads Ultrapure as recommended by manufacturer, and then submitted to immunomagnetic depletion using an auto MACS separator (Miltenyi Biotec). After depletion, cell suspensions were prepared in sterile PBS for mice injection. Depletion efficiency was tested in parallel in all experiments by staining samples before depletion and after IgG or NK depletion with other lineage markers (Ter119, CD19, CD4, CD8), CD3 and NK1.1. NK cells were gated as viable, lineage negative, CD3 negative and NK1.1^{high}. For human NK cells depletion, BM was obtained from healthy volunteers after informed consent and in accordance to Institutional policies (1st Department of Medicine - Department of Haematology, First Faculty of Medicine, Charles University in Prague and General University Hospital, Prague, Czech Republic). Fresh BM cells were submitted to mononuclear cell isolation by Ficoll Hypaque density gradient, washed with sterile PBS/20% FBS, stained with 0.25 µg per 10^6 cells of anti-human biotinylated CD3 (MEM-57) and IgG2a (MOPC-173) or CD56 (MEM-188), and then taken to immunomagnetic separation with streptavidin beads. T-cell depletion with CD3 was performed in both IgG and CD56 depleted experimental arms in order to avoid GVHD and improve survival of the recipient mice. In human experiments, CD56 depletion efficiency was tested by staining pre-depletion and post-depletion samples with CD45, CD19, CD3, CD56 (Figure S4). Serial cell dilutions were prepared in sterile PBS for injection into mice.

Xenotransplantation

NK cell-depleted (CD56) or non-depleted (IgG) human grafts were transplanted into sublethally irradiated (200 cGy) NOD.Cg-*Prkdc*^{scid}*Il2rg*^{tm1Wjl}/SzJ (NSG) mice at different doses. The percentages of human CD45$^+$ cells in the murine blood (8 and 14 weeks) and BM (14 weeks) after transplantation were determined.

Mobilized blood transplantation and IFNγ treatment

NOD.Cg-*Prkdc*^{scid}*Il2rg*^{tm1Wjl}/SzJ (NSG) mice were transplanted with 2 x 10^6 human mobilized blood cells containing an equivalent of 3.6 x 10^5 CD34+ cells. Mice were treated at day 0, 3, 7, 10, and 14 after transplantation with 100 µg murine anti-human IFNγ neutralizing monoclonal antibody (clone NIB42, Exbio, Czech Republic) or murine isotype control IgG1 monoclonal antibody (clone PPV-06, Exbio, Czech Republic). Engraftment was determined at day 17 after transplantation by assessing the percentage of human CD45+ and human CD34+ cells in the BM.

SUPPLEMENTAL REFERENCES

Chen, E.Y., Tan, C.M., Kou, Y., Duan, Q., Wang, Z., Meirelles, G.V., Clark, N.R., and Ma'ayan, A. (2013). Enrichr: interactive and collaborative HTML5 gene list enrichment analysis tool. BMC bioinformatics *14*, 128.

Melenovsky, V., Benes, J., Skaroupkova, P., Sedmera, D., Strnad, H., Kolar, M., Vlcek, C., Petrak, J., Benes, J., Jr., Papousek, F.*, et al.* (2011). Metabolic characterization of volume overload heart failure due to aorto-caval fistula in rats. Molecular and cellular biochemistry *354*, 83-96.